STATIC VOLTAGE STABILITY ASSESSMENT OF NAIROBI AREA POWER DISTRIBUTION NETWORK

SAMUEL AlAL OKETCH

MASTER OF SCIENCE IN ELECTRICAL AND ELECTRONICS ENGINEERING

JOMO KENYATTA UNIVERSITY OF AGRICULTURE AND TECHNOLOGY

2015

Static voltage stability assessment of Nairobi area power distribution network

Samuel Alal Oketch

A thesis submitted in partial fulfillment for the degree of Master of science in Electrical and Electronics Engineering in the Jomo Kenyatta University of Agriculture and Technology

2015

DECLARATION

This thesis is my original work and has not been presented for a degree in any other university.

Signature…….. Date…….....

Samuel A. Oketch

This thesis has been submitted for examination with our approval as University supervisors:

Signature……..... Date…….....…

Dr. Christopher M. Muriithi

JKUAT, Kenya

Signature……. Date……

Dr. Keren K. Kaberere

JKUAT, Kenya

DEDICATION

I dedicate this thesis to my mother and my wife, Martha, my children and to the memory of my late father.

ACKNOWLEDGEMENT

I would like to express my sincere gratitude to my supervisors, Dr. C.M Muriithi and Dr. K.K Kaberere for their guidance, encouragement and constructive suggestions throughout my study. Without their understanding, this thesis would not have become a reality.

I thank Dr. Eng. Wilson Osoro, Eng. Stanley Mutwiri, Eng. Simon Mwangi, Eng. Michael Adhiambo and Eng. Ezra Ndenderu for their support.

I wish to thank Prof. Konditi, Prof. Nderu, the Late Philip Anangi, and Dr. Kihato for encouragement and support.

I wish to thank my colleagues and friends at KPLC, in particular Engineers at Central Design, ESRP, EIU, Energy Transmission based at Kamburu hydro-power station, System Control Nairobi Area, and the O&M Nairobi Region, for their support and understanding.

I wish to thank the staff at KPLC library for their support and understanding. Special thanks to Agnes Wati.

I wish to thank staff at JKUAT library for their understanding and support.

Last but not least, I wish to thank all who worked with me in one way or another, but their names are not listed above. Without your contributions, this thesis would not have become a reality.

TABLE OF CONTENT

LIST OF TABLES

LIST OF FIGURES

LIST OF APPENDICES

LIST OF ABBREVIATIONS

DPL	DigSILENT Programming Language
EHV	Extra High Voltage
FACTS	Flexible A.C. Transmission Systems
HVDC	High Voltage Direct Current
IPPs	Independent Power Producers
KCL	Kirchhoff's Current Law
KENGEN	Kenya Electricity Generation
KPLC	Kenya Power &Lighting Company
LTC	Load Tap changer
MVA	Mega Volt Ampere
MVAr	Mega Volt Ampere Reactive
MW	Mega Watts
OLTC	On load tap changers
ODEs	Ordinary differential equations
p. u	Per unit
SVC	Static VAr Compensators
ULTC	Under Load Tap Changers
VAr	Volt ampere reactive
VS	Voltage Stability

LIST OF SYMBOLS

α	Active power load exponent
β	Reactive power load exponent
δ	Power Angle
I	Current
J	Jacobian Matrix
P	Active Power
Q	Reactive Power
$\|V\|$	Voltage Magnitude
Y	Admittance
X	System Reactance

ABSTRACT

Voltage instability is a problem of overloaded systems. The main factor causing voltage instability is the inability of the power system to meet the demand for reactive power. The Nairobi Area Power distribution network supplies over 50% of Kenya's national load demand. The increase in load demand in the network, over the years has generated interest to the network's voltage stability status. This research assessed the voltage stability of Nairobi Area Power distribution network using static analyses methods. The objectives of the study were to identify the voltage weak buses and overloaded branches in the network, and to assess the network proximity to voltage collapse point. The network power flow problem was formulated, and solution attained using Newton Raphson method to determine the base operating voltages and angles, the power flows, and to compute the full Jacobian matrix. Sensitivity and modal analyses methods were then used to investigate the network weak buses and overloaded branches. Further P-V and Q-V curves analysis methods were used to compute the active and reactive power margins respectively of the identified weak buses.The peak load conditions of June, 2012 were used in the case study. The study established that the network isoperating closer to voltagestabilitylimit at peak load conditions. Further analysis is recommended on thebuses identified as weak to investigate the impact of reactive power compensation, and contingency analysis for the network branches identified as overload to study the impact of loss of any of those branches. Finally, since the loading and network topology of the distribution networks are known to change relatively fast, it is recommended that voltage stability analysis be conducted at regulartime intervals to determine the stability status of the network as the topology and loadings change.

CHAPTER ONE
INTRODUCTION

1.1 Background

In the recent past, the existing distribution networks have witnessed large growths in the network-loads, which have necessitated the need to increase the transfer capacity. The challenges caused by the environmental and economic considerations on the other hand have led to a situation where utilities operate power systems relatively closer to voltage stability limits (Khami et el, 2010). As the system becomes more complex and heavily loaded, voltage instability becomes increasingly serious problem. Under such operating conditions, small incremental changes in loading levels or a contingency may push the system towards the voltage collapse point, a situation which requires urgency of immediate action.

Voltage instability is known to be a problem of the stressed networks. The main factor causing instability is the inability of the network to meet the demand for reactive power (Kundur, 1994; Ajjarapu, 2006; Cutsen and Vournas, 2008).

The initiating event for voltage collapse incident can be due to variety of causes (Kundur, 1994; Ajjarapu, 2006; Cutsen and Vournas, 2008): natural increase in system loads, sudden disturbances such as loss of generating units or heavily loaded lines. When transport of reactive power from neighbouring areas is difficult, any change that calls for additional reactive support may lead to voltage collapse.

Voltages which lie outside the normal operating range due to a disturbance, an increase in system load or change in topology of the system can be an indicator of occurrence of voltage instability. However, the actions of the distribution-level load compensating devices and the limitations in the generator's reactive power capability may precede voltage instability phenomenon without any indicative signs (Zerva, 2010). Hence systems which are heavily loaded could possibly be led to voltage collapse, despite the relatively normal voltage levels within the system.

A simple power system may be considered to consist of the generation units feeding power transformers through transmission lines, to the consumer regions (Cutsen and Vournas, 2008). The voltage collapse is a result of accumulative processes involving actions and interactions of many devices, controls and protective systems in the system.

In a typical voltage collapse scenario, when a disturbance (e.g. an impedance increase) occurs in the network, the primary voltage as seen by the power transformer will initially drop. At this point the power consumed by the load will be less than that corresponding to secondary referencevoltageand LTC will react by decreasing the tap ratio to boost the secondary side voltage (Cutsen and Vournas, 2008).

With each tap operation, the resultant increment of load in the primary voltage lines would cause greater drop in the high voltage levels, due to increase in the line I^2X and I^2R losses, and push the transformer tap settings to the limit (Kundur, 1994; Cutsen and Vournas, 2008).

As a result, with each tap operation, the reactive power output of generators throughout the network would increase.Gradually the generators would hit their reactive power limits (imposed by the maximum allowable field current) one by one. When the first generator reaches its field current limit, its terminal voltage would drop. At reduced terminal voltage fora fixed active power output, the armature current would increase.This may furtherlimit reactive power output to keep the armature current within allowable limits. Its share of the reactive loading would be transferred to other generators, leading to overloading of more and more generators. With fewer generators on the automatic excitation control, the network would be much more prone to voltage instability. This would likely be compounded by the reduced effectiveness of the shunt compensators at low voltages (Kundur, 1994;Cutsen and Vournas, 2008).The process would eventually lead to voltage collapse or avalanche, possibly leading to loss of synchronism in generating units and a major black out.

Incidents of power blackouts due to voltage collapse have been reported in various parts of the world, in the recent past (Kundur, 1994; Ajjarapu, 2006; Cutsen and Vournas, 2008). These incidents were reported to have contributed to adverse impacts on the

economies and lives of the people of the countries concerned. Thus, voltage stability has become a major concern for utilities in power system planning and operation.

Voltage stability analysis in a given system state involves the examination of the factors contributing to instability, the reasons for instability, the voltage weak areas in the network, the system proximity to voltage collapse, and effective ways of improving it (Kundur, 1994;Cutsen and Vournas, 2008; Kothari, 2008).

Since the system dynamics that influence voltage stability are usually slow, many aspects of the problem can be effectively analyzed by static analysis methods which examine the viability of the equilibrium points specified by the given operating point of power system (Kundur, 1994).

The interconnected system in Kenya has a total installed capacity of 1,533 MW made up of 761MW of hydro, 525 MW of thermal, 198 MW of geothermal, 5.45 MW of wind, 26MW of cogeneration and 17MW of isolated grid. Hydro accounts for 50% of the total energy supply. The existing transmission network consists of 220kV and 132kV high voltage transmission lines, and the distribution network consists of 66kV feeder lines around Nairobi and the 33kV and 11kV medium voltage lines. The existing transmission and distribution network lengths currently are estimated as follows: about1, 331km of 220kV, about 2,211km of 132kV, about 655km of 66kV, about 13,812km of 33kV and about 25,485km of 11kV lines (LCPDP, 2011).

Through the initiatives by the Government of Kenya, i.e.the Energy Access scale up program, the national demand for Electricity has shown an upward trend in the recent past. While the demand was 4,200GWh in 2004/05 (LCPDP, 2011), it has risen to the current Figure of 5,639GWh.

Nairobi area has consistently recorded the highest sales in electricity in Kenya, accounting for more than 50% of the total sales. Under the same review period, the sales increased from 2,334GWh in 2004/05 (LCPDP, 2011) to current Figure of 3,019GWh.

1.2 Problem Statement

The Nairobi area Power Distribution Network supplies over 50% of Kenya's national load demand (LCPDP, 2011). The network has over the years witnessed large growths in

load demand without a corresponding enhancement of the network distribution facilities(lines, substations, bus bars etc.),which implies that it could be operating close to its voltage stability limit, and this is what generated interest to analyze its voltage stability status.

Under such operating circumstances, the voltage collapseincidents could occur in the network as a result of small incremental changes in the loading levels or a contingency.To the best of the authors' knowledge, there is no literature available focusing on the status of the voltage stability of the Kenyan'sdistribution systems. Therefore, the needarose to conduct a comprehensive studyto establish the voltage stability status of the network, and to develop measures that can be applied to prevent the possibility of occurrence of voltage collapse.

1.3 Main Objective

The main objectives of this study are to identify the load buses and branches which arepronetovoltage collapse, using the *QV* Modal and *VQ* Sensitivity analyses methods, and to assess the network proximity to voltage collapse point using *PV* and *QV* curves analyses methods.

The *QV* modal and *VQ* sensitivity analysis methods are reducedJacobian matrix based indicators. The power flow Jacobian matrix is reduced to the first derivative of reactive power equations in relation to the voltage magnitude by assuming that the generator and load buses present no active power variations. The bus sensitivities are studied by analyzing the inverse of the reduced Jacobian matrix.

1.4 Specific Objectives

(i) To model Nairobi Area Power Distribution Network, perform power flow analysis, and to establish the network base case operating conditions (see Figure 3.1).

(ii) To identify the voltage weak buses and overloaded branches, where voltage collapse initiating events could occur, using the *VQ* sensitivity and *QV* modal analyses methods.

(iii)To assess the network proximity to voltage collapse point using *PV* and *QV* curves analysis methods, and recommend remedial measures.

1.5 Scope of the Study

This study was conducted on the 66kV network of the Nairobi Area Distribution network. The network was modeled as it existed by June, 2012, and the study is based on the peak load conditions of the same period.

1.6 Contributions of the Thesis

1.6.1 Published Conference Proceedings

a) *Oketch S. A., Muriithi C. M., Kaberere K. K,* 'Static Voltage Stability Analysis of Nairobi Area Power Distribution Network', Proceedings, 15th -17thAugust, 2012 Kenya Society of Electrical & Electronics Engineering and Japanese Society of Electrodynamics and Mechanics conference, Jomo Kenyatta University of Agriculture & Technology (AICAD)

b) *Oketch S. A., Muriithi C. M., Kaberere K. K.,* 'Voltage Stability Assessment of Nairobi Area Power Distribution Network Using P-V and Q-V curves', Proceedings, 24th – 26th April, 2013 Sustainable Research Innovation Conference,Jomo Kenyatta University of Agriculture & Technology (ICAD)

c) *Oketch S. A., Muriithi C. M., Kaberere K. K,* ''Investigating Voltage Stability of Nairobi Area Power Distribution Network'', Proceedings, 4th-5th September, 2013 Kenya Society of Electrical & Electronics Engineering and Japanese Society of Electrodynamics and Mechanics conference, Dedan Kimathi University of Technology, Nyeri.

1.6.2 JournalPaper Submitted For Publication

Oketch S. A., Muriithi C. M., Kaberere K. K, "Static Voltage Stability Analysis of Nairobi Area Power Distribution Network"`, Journal of Applied Sciences, Engineering and Technology forDevelopment (JASETD), Dedan Kimathi University of Technology, Nyeri

CHAPTER TWO
LITERATURE REVIEW

2.1 Introduction

Power system stability is defined as the characteristic of the power system to remain in state of equilibrium at normal operating conditions and to restore an acceptable state of equilibrium after a disturbance (Kundur, 1994; Ajjarapu, 2006; Cutsen and Vournas, 2008). Power system stability is divided into voltage stability frequency stability and rotor angle stability. Frequency stability is the ability of power system to compensate for power deficit. Rotor angle stability is the ability of inter connected synchronous machines of power system to remain in synchronism. The rotor angle stability is divided into small signal and transient stability.Real power is related to rotor angle instability. Similarly reactive power is central to voltage instability analysis (Kundur, 1994; Ajjarapu, 2006; Cutsen and Vournas, 2008; Kothari, 2008). This research work is on voltage stability.

This chapter presentsliterature review on voltage stability and introduces the definitions, classifications, and the factors that influence voltage instability. The chapter also introduces the voltage stability analysis methods, characteristics of reactive compensating devices, and methods for prevention of voltage collapse.

2.2 Definition of Terms

2.2 1 Voltage Stability

Voltage stability is the ability of power system to maintain steady acceptable voltages at all the buses in the system at normal operating conditions and after being subjected to disturbances (Kundur, 1994; Ajjarapu, 2006; Cutsen and Vournas, 2008; Kothari, 2008). A power system is voltage stable if voltages after a disturbance are close to voltages at normal operating conditions.Voltage instability may also be defined as a limiting stage beyond which the reactive power injection does not elevate the system voltage to normal (Das, 2006).

Voltage instability stems from attempt by load dynamics to restore power consumption beyond the combined capability of the transmission and generation system (Kundur, 1994; Ajjarapu, 2006; Cutsen and Vournas, 2008). The main factor causing the instability is the inability of the power system to meet the demands for reactive power in a heavily stressed system to keep the desired voltage levels.

A criterion for voltage stability is that at a given operating condition for every bus in the system, the bus voltage magnitude increases as the reactive power injection at the same bus is increased. A system is voltage unstable if for at least one bus in the system, the bus voltage magnitude (V) decreases as the reactive power injection (Q) at the same bus increases. In other words, a system is voltage stable if VQ sensitivity is positive and voltage unstable if VQ sensitivity is negative for at least one bus (Kundur, 1994). Voltage control and instability are local problems. However, the consequence of voltage instability can have widespread impact.

2.2.2 Voltage Collapse

Voltage collapse is the process by which the sequence of events accompanying voltage instability leads to unacceptable voltage profile in a significant part of power system (Kundur, 1994; Cutsen and Vournas, 2008). The accompanying events may involve the actions and interactions of many devices, controls and protective systems. Following voltage instability, a power system undergoes voltage collapse if the post-disturbance equilibrium voltages near loads are below acceptable limits (Kothari, 2008). The Voltage collapse may be total (blackout) or partial.

The voltage collapse generally manifests itself as a slow decay of voltage profiles. The duration of voltage collapse dynamics is of the order of few seconds to several minutes. Voltage collapse is influenced by system conditions and characteristics. The following are significant factors contributing to the instability and/or collapse (Kundur, 1994; Cutsen and Vournas, 2008): Large distances between generation and load; ULTC action during low voltage conditions; Unfavorable load characteristics; Poor coordination between various control and protective systems. Voltage collapse may be aggravated by the excessive use of shunt capacitor compensation.

2.3 Classification of Voltage Stability

Voltage stability, in the context of power system stability may be classified based upon two criteria: time scale and driving force of instability as shown in table 2.1 (Kundur, 1994; Ajjarapu, 2006; Cutsen and Vournas, 2008).

Table 2.1: Classification of power system stability, source :(Cutsen and Vournas, 2008)

<table>
<tr><td>Time scale</td><td colspan="2">Generator driven</td><td colspan="2">Load driven</td></tr>
<tr><td rowspan="2">Short term</td><td colspan="2">Rotor angle stability</td><td colspan="2" rowspan="2">Short term voltage stability</td></tr>
<tr><td>Small signal</td><td>Transient</td></tr>
<tr><td rowspan="2">Long term</td><td colspan="2" rowspan="2">Frequency stability</td><td colspan="2">Long term voltage instability</td></tr>
<tr><td>Small disturbance</td><td>Large disturbance</td></tr>
</table>

The voltage stability is load driven problem and is divided into short term and long term voltage stability based on the time scale of load component dynamics (Ajjarapu, 2006; Cutsen and Vournas, 2008). For the purpose of analysis, voltage stability can also be classified as small and large disturbances. This study analyzed voltage stability of the Nairobi Area distribution network at peak load conditions.

2.3.1 Short Term Voltage Stability

Short term voltage instability often may occur if loads are composed of a large number of induction machines, and an event such as a contingency or rapid load increase, causes bus voltages to decline sufficiently to cause a number of induction motors to stall (Kundur, 1994; Ajjarapu, 2006; Cutsen and Vournas, 2008).

In short term voltage stability the driving force of instability is the tendency of the dynamic loads to restore consumed power in the time frame of a second. A typical load component of this type is the induction motor and also an HVDC link with first power control (Kundur, 1994; Ajjarapu, 2006; Cutsen and Vournas, 2008).

The analysis of short term voltage instability requires the use of time domain simulations since the dynamics of the load and system controls (which cannot be adequately studied by steady state analysis) determine whether the system will be stable or unstable (Morison et el, 2006; Cutsen and Vournas, 2008). The time scale for short term voltage stability is in the order of several seconds.

2.3.2 Long Term Voltage Stability

Long term voltage instability occurs if the system has survived short term period following the initial disturbance (Kundur, 1994; Ajjarapu, 2006; Cutsen and Vournas, 2008).

As voltages decline in a system, a number of controls will act to restore voltages close to their pre-contingency levels. Such controls include generator AVRs, static VAr systems (SVS), automatic switched capacitors, and automatic transformer under load tap changers (ULTCs). As the voltage is raised, loads begin to be restored to pre contingency MW and MVAr levels. This increases reactive losses through the system, and puts additional reactive demand on the already weakened system. Eventually the ability to provide more reactive support will be curtailed as (a) generator over excitation limiters act, (b) SVCs may reach their maximum outputs, (c)all available switchable capacitor banks will be exhausted. As reactive supply is curtailed, the system voltage will drop further aggravating the condition, since the support from the static capacitors will drop and induction motors will draw more reactive power, or actually stall. The time of long term voltage instability could extend from few tens of seconds to few minutes (Kundur, 1994; Ajjarapu, 2006; Morison et el, 2006; Cutsen and Vournas, 2008).

2.3.3 Small Disturbance Voltage Stability

Small disturbance voltage stability considers the power systems ability to control voltages after a small disturbance, e.g. changes in load. The analysis of small disturbance voltage stability is done in steady state. In that case the power system is linearized around an operating point and the analysis is done using eigenvalues and

eigenvectors techniques (Kundur, 1994; Ajjarapu, 2006; Cutsen and Vournas, 2008). This form of stability is influenced by characteristics of loads, continuous controls, discrete controls at the given instant of time.

2.3.4 Large Disturbance Voltage Stability

This is the ability of power system to maintain steady voltages following a large disturbance such as system faults, loss of generation or other contingencies (Kundur, 1994; Ajjarapu, 2006; Cutsen and Vournas, 2008). Determination of this form of stability requires examination of dynamic performance of the system over the period sufficient to capture the interaction of such devices as ULTCs and generator field current limiters. The study period of interest may extend from a few seconds to tens of minutes. Large Disturbance Voltage Stability can be studied by using nonlinear time domain simulations which include proper modeling of the network under study.

2.4 Factors Influencing Voltage Stability

Voltage stability problem normally occurs in heavily stressed systems. In addition to the strength of transmission line and power transfer levels, the principle factors contributing to voltage collapse are generator reactive power/voltage control limit, load characteristics, characteristics of reactive compensating devices and action of voltage control devices such as transformer load tap changers (LTCs) (Kundur, 1994; Ajjarapu, 2006; Cutsen and Vournas, 2008).

2.4.1 Reactive Power Control Devices

Reactive power flows can give rise to substantial voltage changes across the system, which means that it is necessary to maintain reactive power balances between sources of generation and points of demand (Kundur, 1994; Cutsen and Vournas, 2008; Das, 2011; Chakrabarti, 2012). Some of the devices and strategies available for reactive power compensation and control are: Synchronous machines; synchronous condensers; shunt capacitors and reactors; static VAr controllers; Series capacitors with PSSs (power system stabilizers); Line dropping; under voltage load shedding; Voltage reduction; under load tap changing transformers; setting lower transfer limits.

2.4.1.1 Action of Load Tap Changers

One of the key mechanisms in load restoration is the voltage regulation performed automatically by the tap changing devices of the main power delivery transformers. The tap changer controls the voltage of the distribution medium voltage (MV) side by changing the transformer ratio r (Cutsen and Vournas, 2008).

In most cases the variable tap is on the high voltage (HV) side. One reason for that is the current is lower at this side making insulation requirements less. Another reason is that more turns are available at the HV side making regulation more precise. Exceptions to this rule can be found mostly in case of autotransformers (Cutsen and Vournas, 2008).

Two types of tap-changing facilities are provided: the off-load tap changing and the under load tap changing (ULTC). The off-load tap changing facilities require the transformer to be de-energized for tap changing; they are used when the ratio will need to be changed to meet the long term variation due to load growth, system expansion or seasonal changes. The ULTC is used when changes in ratio need to be frequent, for example to take care of daily variations in system conditions (Kundur, 1994; Cutsen and Vournas, 2008).

The minimum time required for tap changer to complete one tap movement is usually close to 5 seconds (mechanical time delay, τ_m). Various intentional time delays (ranging from several seconds to a couple of minutes) are usually added to mechanical time delay to avoid frequent or unnecessary tap movement, which are a cause of wear and tear to the equipment. The intentional time delays are either constant or variable. In the latter case, the inverse time characteristic is used because the time delay becomes shorter for larger voltage errors.

One important constraint of LTC is that the variable tap ratio has a limited regulation range

$$r^{min} \leq r \leq r^{max}$$

Typical values of the lower limit are from 0.85-0.9 p.u and for the upper limit 1.10-1.15 p.u. and the size of a tap step is usually in the range 0.5%-1.5% (Cutsen and Vournas, 2008).

Figure 2.1 illustrates the load restoration through LTC operation using a simple system which consists of a generator feeding an LTC transformer through a transmission line. The LTC is shown as an ideal transformer in series with a leakage reactance. P_1, Q_1 are the active and reactive powers absorbed by the transformer, and $P(V_2)$, $Q(V_2)$ the dynamic loads at the distribution end.

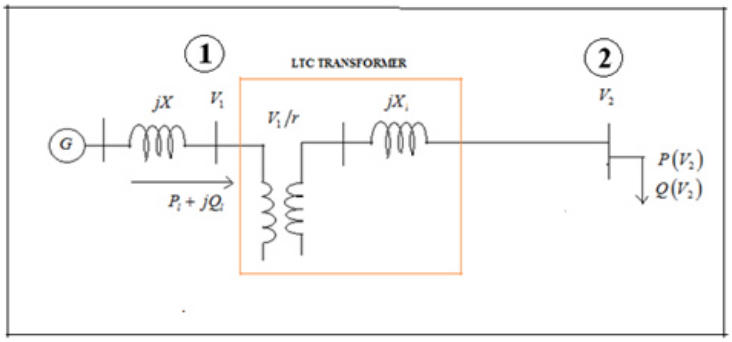

Figure 2.1: Generator-Line LTC system, Source: (Cutsen and Vournas, 2008)

Two network P_1V_1 characteristics relating the transmission side voltage V_1 to the power P_1deliveredto the transformer are shown in Figure 2.2. The network characteristic is drawn for the P_1Q_1 pairs corresponding to the load connected at bus 2.

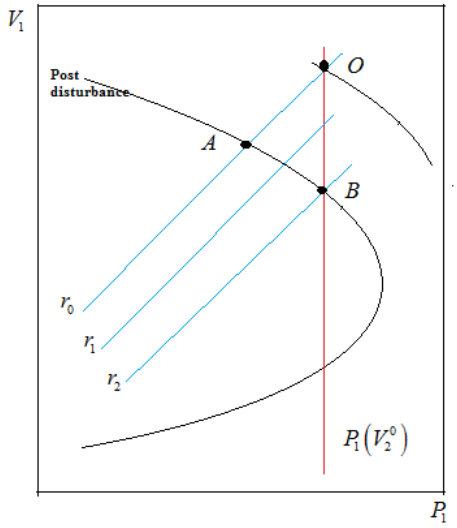

Figure 2.2: PV curve of generator-LTC characteristics:
Source (Cutsen and Vournas, 2008)

To illustrate the LTC operation, let us assume the system is initially operating at point O in Figure 2.2, when a disturbance (e.g. an impedance increase) forces the network characteristics to the post disturbance one. The primary voltage V_1 will initially drop along the transient LTC load characteristic for a given value of $r = r_o$ from point O to point A. At this point the power consumed by the load is less than that corresponding to secondary reference voltage, V_2^o meaning that $V_2 < V_2^0$. Since V_2 is less than the reference, the LTC will react by decreasing the tap ratio to boost the secondary side voltage. This will change the transient load characteristics, and the operating point will move along the post disturbance network characteristic, until the new operating characteristics is found close to point B, where the steady state load characteristics intersects the network characteristics. Note that during this operation, the LTC is restoring both the secondary voltage and load power (Cutsen and Vournas, 2008). The tap changer actionresults in the increment of load in the primary voltage lines, which causes increase the line I^2X and I^2R losses, and in turn results in greater drop in the high voltage levels, and push the transformer tap settings to the limit. During the restoration process, the increase in load demandresults in decrease of the network load impedance.

2.4.1.2 Load Characteristics

The exponential load characteristic has the following general form: (Cutsen and Vournas, 2008).

$$P = zP_O\left(\frac{V}{V_O}\right)^{\alpha} \tag{2.1}$$

$$Q = zQ_O\left(\frac{V}{V_O}\right)^{\beta} \tag{2.2}$$

Where z is a dimensionless demand variable, V_o is a reference voltage and the exponents $\boldsymbol{\alpha}$ and $\boldsymbol{\beta}$ depending on the type of load (motor, heating, lighting etc).

zP_o and zQ_o are the active and reactive powers consumed under a voltage V equal to reference V_o and relate to the amount of connected equipment.

$\alpha=\beta=2$: Constant impedance load (often called z)

$\alpha=\beta=1$: Constant current load (often called I)

$\alpha=\beta=0$: Constant power load (often called P)

With constant impedance static load characteristics, the system stabilizes at power and voltage levels lower than desired values (Cutsen and Vournas, 2008). With constant power load characteristics, the system becomes unstable through collapse of load bus voltages.With other characteristics the voltage is determined by the composite characteristic of transmission line and load.

Care should be taken when using the exponential loads at low voltage levels, because when voltage drops below threshold value (e.g. $V<0.6$) many loads may be disconnected, or may have their characteristics completely altered (Cutsen and Vournas, 2008).

The load characteristic becomes a polynomial in V if all the exponents are integer. A special case is the *ZIP* model, which is made up of three components, constant impedance, and constant current and constant power. The real and reactive characteristics of *ZIP* load models are given by the following quadratic expressions:

$$P = zP_O\left[ap\left(\frac{V}{V_o}\right)^2 + bp\frac{V}{V_o} + cp\right] \quad (2.3)$$

$$Q = zQ_O\left[aq\left(\frac{V}{V_o}\right)^2 + bq\frac{V}{V_o} + cq\right] \quad (2.4)$$

Where P, Q are active and reactive powers respectively, drawn at the particular bus; P_o, Q_o are the active and reactive powers respectively drawn at that bus at the initial system state; ***ap, bp, cp and aq, bq and cq*** are fractional portions of the power representing constant impedance, constant current and constant power respectively with their sum equal to 1.0

The *ZIP* model is unrealistic for low voltages because some of the polynomial loads parameters, usually the ones defining current contributions ***bp*** (or ***bq***) may assume negative values, especially when they are obtained from measurements (Cutsen and Vournas, 2008).

The power consumed by loads depends on their voltage characteristics. This dependence may be permanent in which case the load is purely static, or it may change with time, in which case the load is dynamic.

The dynamics of various load components and control mechanisms tend to restore load power, at least to a certain extent. This is referred to as load restoration (Cutsen and Vournas, 2008).

Figure 2.3 shows the load and network *PV* curves. The load characteristics interact with the network characteristics to produce the operating point of the system for the various changes in demand.

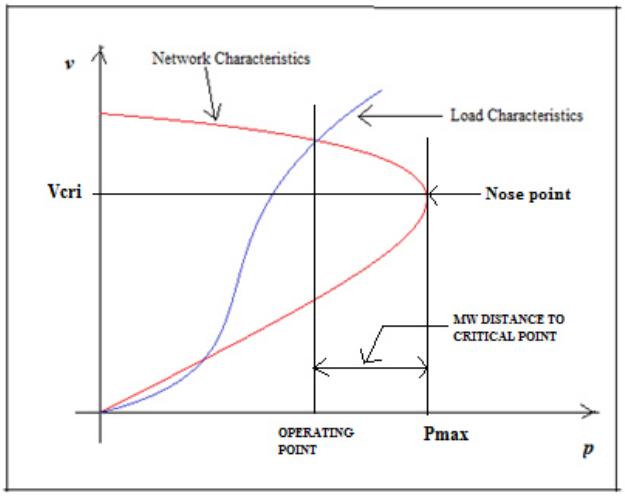

Figure 2.3: Load and Network PV curves: source (Cutsen and Vournas, 2008).

An obvious prerequisite to stable system operation is the existence of equilibrium, given by the intersection of both characteristics. Voltage instability may be caused by changes in system parameters that lead to the disappearance of an equilibrium.

Figure 2.4(a) illustrates an instability scenario mechanism where an increase in load demand causes the load equilibrium characteristics to change so that it does not interact with the network characteristics.

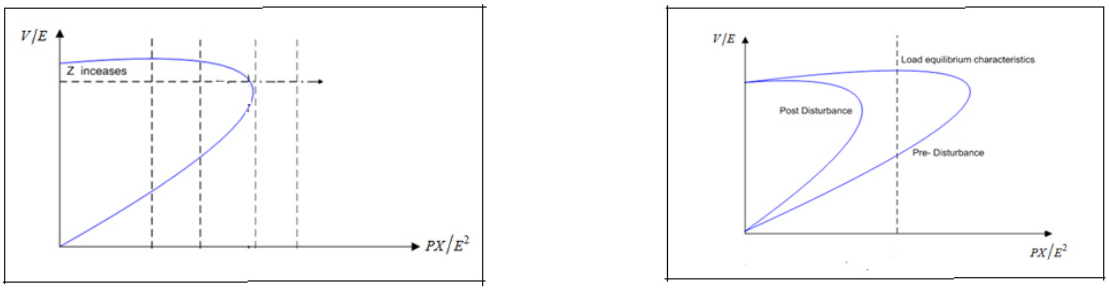

(a) (b)

Figure 2.4: Instability mechanism illustrated by PV, load equilibrium characteristics with *α=β=0: source* (Cutsen and Vournas, 2008).

Figure 2.4(b) illustrates an instability caused by a large disturbance, e.g. loss of transmission *and/or* generation equipment. The disturbance causes the network characteristics to shrink drastically so that the post disturbance *PV* curve does not intersect (the unchanged) load characteristic resulting in voltage collapse in the post disturbance network.

In Figure 2.5 the same two scenarios is illustrated for a load characterized by ***α=β=0.7*** instead (***α=β=0***) at equilibrium.

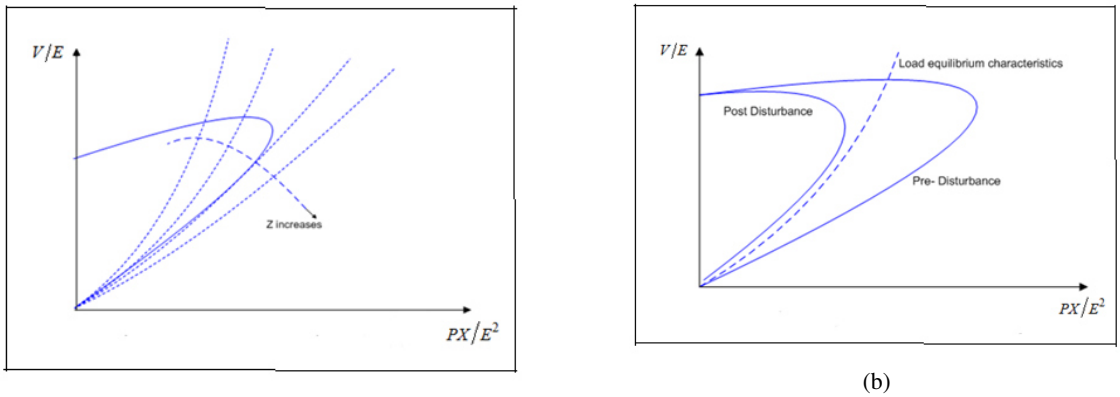

(a) (b)

Figure 2.5: Instability mechanism illustrated by PV, load equilibrium characteristics with *α=β=0.7: source (Cutsen and Vournas, 2008).*

Assuming a smooth load increases as in Figure 2.4(a) and 2.5(a), the point where the load characteristics becomes tangent to the network characteristics defines the loadability limit of the system. A load increase beyond the loadability limit results in the loss of equilibrium and the system can no longer operate. In Figure 2.4(a) the point where the load and the network *PV* curves are tangent coincides with the maximum deliverable power, because load is assumed to restore to constant power. However, the loadability limit does not necessarily coincide with the maximum deliverable power since it depends on the load characteristics.This can be seen from Figure 2.5 (a). For certain load characteristics, there is no loadability limit, i.e. there is an operating point for all the demands. However some of these operations may be infeasible for other reasons such as unacceptably low voltages (Cutsen and Vournas, 2008).

2.4 Countermeasures against Voltage Instability

At power system planning stage, transmission reinforcement is the most obvious choice. However environmental considerations leave little room for new transmission lines near heavily populated load centers, so that other solutions must be sought (Cutsen and Vournas, 2008).

In designing system protection against voltage instability, load reduction is always the ultimate countermeasure. The system protection scheme has to be designed complementary to, and in coordination with equipment protection such as that of generators, or transmission lines (Cutsen and Vournas, 2008).

During normal operation, real time control involves typically generator *AVR* set point modification, reactive device switching, generator rescheduling, etc. These actions are usually performed manually by system operators. Alternatively in some countries, some of them are implemented automatically through the secondary voltage control (Cutsen and Vournas, 2008).

When a power system is prone to short term voltage instability (large induction motor loads and/ or HVDC system fed from weak AC system) fast reactive support near the load center is essential. The most common fast reactive support devices are generators, synchronous condensers and SVCs (Cutsen and Vournas, 2008). The other remedies for

short term voltage instability are the fast automatic undervoltage load shedding and selective load shedding, while in case of instabilities caused by transient faults, a fast fault clearing mechanisms is recommended.

For the long term voltage instability, remedial action objectives are achieved by using variety of control actions, such as reactive compensating switching, generation scheduling or load reduction [3].Load reductioncan be achieved either by directshedding or indirectly through emergency LTC control. The LTC emergency controls are implemented by LTC blocking,which bring back the tap to a predetermined position, or by reducing LTC set point, the actions of whichslows down system degradation by stopping the load restoration process. For multilevel LTC systems, the emergency control actions at different levels must be coordinated (Cutsen and Vournas, 2008). The other countermeasure available when there is some reactive generation reserve is the boosting of generator terminal voltages.

2.5 Analysis of Voltage Stability

This section presents some of the static analysis tools used in this study to analyze voltage stability status of a distribution network. These tools are sensitivity and modal analyses methods and Q-V and P-V curves methods.

2.5.1 V-Q Sensitivity Analysis

The power flow problem can be formulated as (Kundur, 1994; Hasani and Parniani, 2005; Khami et el, 2010; Althowibi and Mustafa, 2010; Mustapha and Murugesan, 2011; Chakrabati and Halder, 2012).

$$\begin{bmatrix} \Delta P \\ \Delta Q \end{bmatrix} = \begin{bmatrix} J_{P\delta} & J_{PV} \\ J_{Q\delta} & J_{QV} \end{bmatrix} \begin{bmatrix} \Delta \delta \\ \Delta V \end{bmatrix} \qquad (2.5)$$

Where ΔP and ΔQ are the incremental changes in bus active and reactive powersrespectively, $\Delta \delta$ and ΔV are the incremental changes in the bus voltage angle and magnitude respectively, and

$\begin{bmatrix} J_{P\delta} & J_{PV} \\ J_{Q\delta} & J_{QV} \end{bmatrix}$ is the Jacobian matrix

The *i-th* diagonal element of the matrix $[J_{QV}]$ is the Q-V sensitivity of the load bus-*i*, considering changes both in real and reactive bus powers, i.e.

$$\frac{dQ_i}{dV_i} = [J_4]_{ii}$$

However at each operating point, we may keep *P* constant and evaluate voltage stability by considering the incremental relation between *Q* and *V*. Although incremental changes in *P* are neglected in the formulation, the effect of changes in system load or power transfer level is taken into account by studying the incremental relationship between *Q* and *V* at different operating conditions (Kundur, 1994).

The linearized power flow equationis expressed by equation (2.5).In this expression,

$$\Delta P = 0, \quad [\Delta Q] = [J_R][\Delta V] \tag{2.6}$$

Where

$$[J_R] = [J_4] - [J_3][J_1]^{-1}[J_2] \tag{2.7}$$

$[J_R]$ is called the reduced Jacobian matrix of the system.

From equation (2.6)

$$[\Delta V] = [J_R]^{-1}[\Delta Q] \tag{2.8}$$

$J_R^{-1}$is called the reduced *VQ* Jacobian matrix, and its i^{th} diagonal element is the *VQ* sensitivity at bus *i*, which indicates the relationship between the voltage and the imported reactive power at this bus (Kundur, 1994).

The *VQ* sensitivity at a bus represents the slope of *QV* curve at a given operating point, a positive valuebeing indicative of a stable operation and a negative value unstable operation. Whendiagonal element magnitude is positive, the increase of reactive power induces increase of bus voltage, which means the system bus voltage is stable. The smaller the *i-th* diagonal element, the more stable the system (Kundur, 1994). When sensitivity grows, controllability decreases, reaching zero at the verge of stability at which the bus voltage is non-controllable. Thus when the diagonal element magnitude is

negative the increase in reactive power leads to decrease in bus voltage, implying the system is unstable (Kundur, 1994; Mustapha and Murugesan, 2011).

2.5.2 *QV* Modal Analysis

Voltage Stability characteristics of a power system can be identified by computing the eigenvalues and eigenvectors of the reduced Jacobian matrix, J_R defined by equation (2.7) (Kundur, 1994; Ellithi et el, 2000; Hasani and Parniani, 2005; Khami et el, 2010; Larki et el, 2010; Althowibi and Mustafa, 2010; Mustapha and Murugesan, 2011; Chakrabati and Halder, 2012).

The Reduced Jacobian Matrix can be presented as:

$$J_R = \xi \Lambda \eta \tag{2.9}$$

Where,

ξ is the right eigenvector matrix of J_R

η isthe lefteigenvector matrix of J_R

Λ is the diagonal eigenvalues matrix of J_R

From equation (2.9),

$$J_R^{-1} = \xi \Lambda^{-1} \eta \tag{2.10}$$

Substituting equation (2.10) in (2.8) gives

$$\Delta V = \xi \Lambda^{-1} \eta \Delta Q \tag{2.11}$$

Or

$$\Delta V = \sum_i \frac{\xi_i \eta_i}{\lambda_i} \Delta Q \tag{2.12}$$

ξ_i is the i^{th} column of the right eigenvector and η_i is the i^{th} row of the left eigenvector. Since $\xi^{-1} = \eta$ equation (2.12) can be represented as:

$$\eta \Delta V = \Lambda^{-1} \eta \Delta Q \tag{2.13}$$

Or

$$v = \Lambda^{-1} q \tag{2.14}$$

Where

$v = \eta \Delta V$ is the vector of modal voltage variations.

$q = \eta \Delta Q$ is the vector of modal reactive variations.

The difference between equations (2.8) and (2.14) is that Λ^{-1}, is a diagonal matrix whereas J_R^{-1} in general, is non-diagonal. Equation (2.14) is a representation of uncoupled first order equations.

Thus, for the i^{th} mode

$$v_i = \frac{1}{\lambda_i} q_i \tag{2.15}$$

The eigenvalues and the corresponding eigenvectors of J_R define different modes of the system. The magnitudes of eigenvalues determine the degree of stability of different modes in the system. As shown in equation (2.15), the magnitude of each modal voltage variation is directly proportional to the magnitude of modal reactive power variation and inversely proportionalto λ_i. If λ_i is positive, this implies the i^{th} modal voltage and the i^{th} modal reactive power variations are in the same direction, indicating that the system is voltage stable. From equation (2.15), the smaller the λ_i, the bigger shall be the modal voltage variations and therefore, the more critical, the mode:When $\lambda_i = 0$, the i^{th} modal voltage collapses because any change in modal reactive power causes infinite change in modal voltage. If λ_i is negative, the i^{th} modal voltage and the i^{th} modal reactive power variations are in the opposite directions indicating that the system is voltage unstable.

It is impractical and unnecessary to calculate all the eigenvalues of J_R for a practical system with several thousand buses (Kundur, 1994). On the other hand, calculating only

the minimum eigenvalue of J_R is not sufficient because there is usually more than one mode associated with different parts of the system, and the mode associated with the minimum eigenvalue may not be the most troublesome mode as the system is stressed. In practice, it is seldom necessary to compute more than 5 to 10 of the smallest eigenvalues to identify all critical modes.

If the transmission network resistance is neglected and node admittance matrix Y_N is symmetrical, the reduced Jacobian matrix J_R is also symmetrical (Kundur, 1994). The eigenvalues and eigenvectors of J_R are real. In addition, the right eigenvector and left eigenvector of an eigenvalue of J_R are equal. With phase shift transformer (which make the matrix Y_N unsymmetrical) and the line resistances, J_R is only nearly symmetrical; the eigenvalues of J_R for all practical purposes are real.

In general, it can be said that a system is voltage stable if the eigenvalues of J_R are all positive. This is different from the dynamic systems where eigenvalues with negative real parts are stable. J_R can be taken as a symmetric matrix and therefore the eigenvalues of J_R are close to being purely real (Enemout et el, 2013).

2.5.2.1 Bus Participation Factors

The determination as to which node or load bus participates in a selected mode isaccomplished byusingbus participation factors, which identify the weakest nodes or load buses that are making significant contribution to the selected modes.

The relative participation of bus k in mode i is given by bus participation factor P_{ki} (Kundur, 1994; Althowibi and Mustafa, 2010; Larki et el, 2010) as:

$$P_{ki} = \xi_{ki}\eta_{ki} \qquad (2.16)$$

The bus participation factor determines the contribution of λ_i to the VQ sensitivity at bus k. A high value of P_{ki} at bus k for mode i means this bus is close to voltage instability in this mode. Therefore bus participation factors can be used to determine weak areas in the system. There are generally two types of modes, localized and non-localized (Kundur, 1994). The localized modes have very few buses with large participations and others

with almost zero value; whereas the non-localized modes have many buses with relatively small participations.

Localized modes are associated with the swinging of units at a generating station with respect to the rest of the power system (Gajjor and Samon, 2012). Oscillations occur only to the small part of the power system. Typically, the frequency range is 1-2 Hz.

Non-localized modes are either intra plant modes or inter-area modes. The intra plant modes are observable only within and near generating plants (Gajjor and Samon, 2012). Typical frequency range is *1.5-3Hz*. The inter area modes are associated with swinging of many machines in one part of the system against machines in other parts. It generally occurs in weak interconnected power systems through long tie lines. Typically frequency range is 0.1-1 Hz.

Over and above these, there are some modes of oscillations associated with controls like HVDC, FACTS and turbine generators.

2.5.2.2 Branch Participation Factors

If we assume vector of modal reactive power variations, q corresponding to mode i to have all elements equal to zero except the i^{th}, which equals to 1, then the corresponding vector of bus reactive power variations is (Kundur,1994):

$$\Delta Q^{(i)} = \eta^{-1} q = \xi q = \xi_{(i)} \tag{2.17}$$

Where ξ_i is the *i-th* right eigenvector of J_R

The vector of bus voltage variations is

$$\Delta V^{(i)} = \frac{1}{\lambda_i} \Delta Q^{(i)} \tag{2.18}$$

The corresponding vector of bus angle variations is

$$\Delta \theta^{(i)} = -J_{P\delta}^{-1} J_{PV} \Delta V^{(i)} \tag{2.19}$$

The linear relationships for the real and reactive powers at a bus can be obtained for small variations in variables θ and V by forming total differentials (Arrilaga and Arnold, 1994) as follows:

For a PQ bus bar

$$\Delta P_k = \sum_{m \in k} \frac{\partial P_k}{\partial \theta_m} \Delta \theta_m + \sum_{m \in k} \frac{\partial P_k}{\partial V_m} \Delta V_m \tag{2.20}$$

$$\Delta Q_k = \sum_{m \in k} \frac{\partial Q_k}{\partial \theta_m} \Delta \theta_m + \sum_{m \in k} \frac{\partial Q_k}{\partial V_m} \Delta V_m \tag{2.21}$$

The power variations at each bus withrespecttobus anglesandvoltages are summed up in their respective segments of the Jacobian matrix. In expressions (2.20) and (2.21):

$\frac{\partial P_k}{\partial \theta_m}$, $\frac{\partial P_k}{\partial V_m}$ refers to $J_{P\delta}$ and J_{PV} respectively in equation (2.5).

$\frac{\partial Q_k}{\partial \theta_m}$, $\frac{\partial Q_k}{\partial V_m}$ refers to $J_{Q\delta}$ and J_{QV} respectivelyin equation (2.5)

$\Delta \theta_m$, ΔV_m are the vectors of bus angle and voltage variations respectively.

For *PV* bus bar, only equation (2.20) is used since Q_k is not specified. For slack bus bar, no equation is used.With angle and voltage variations for both the sending end and the receiving end known, the linearized change in branch reactive loss can be calculated (Kundur, 1994). The relative participation of branch *j* in mode *i* is given by the participation factor:

$$P_{ji} = \frac{\Delta Q_{loss} \ for \ branch \ j}{ma \times imum \ \Delta Q_{loss} \ for \ all \ branches} \tag{2.22}$$

Branch participation factor; indicate for each mode which branches consume the most reactive power in response to an incremental change in reactive load (Kundur, 1994). Branches with high participations are either weak links or are heavily loaded.

2.5.3 Margin Calculation Using *PV* and *QV* curves

At the voltage collapse point, the maximum power transfer limit has been reached, and therefore operation of power system faces difficulties. For a satisfactory operation, a sufficient power margin must be allowed. In assessing the network proximity to voltage collapse point, *PV* and *QV* curves are plotted and analysed (Kundur, 1994; Ellithi et el, 2000; Hasani and Parniani, 2005; Reis et el, 2009; Larki et el, 2010; Gunner and Bilir, 2010; Mustapha and Murugesan, 2011). These two methods define steady state loadability limits which are related to voltage stability.

It has been argued in literature that *QV* curve technique is preferable when determining the reactive supply problems, whereas the *PV* curve analysis is preferable for providing power loading and transfer indications.

2.6.3.1 P-Margin Calculation Using *PV* Curves

The *PV* curve at a load bus is produced by incrementally increasing the active power, *P* and performing series of power flow solutions for the different loading levels, until the maximum power transfer limit is reached (Kundur, 1994). The *PV* curve is plotted using the calculated values of voltages corresponding to the incremental changes of *P* values at the candidate bus. A typical *PV* curve is shown in Figure 2.6.

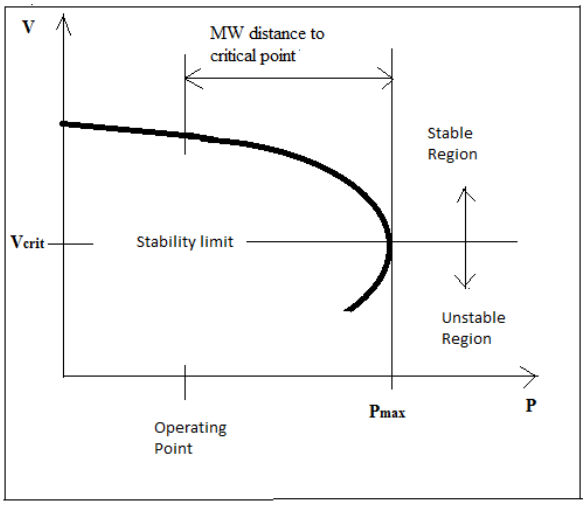

Figure. 2.6: Typical *PV* Curve, source: (Mustapha and Murugesan, 2011)

As shown in Figure 2.6, the real power margin is the Megawatt (MW) distance from the operating point to the voltage collapse point (Kundur, 1994).

2.6.3.2 Q-Margin Calculation using *QV* curves

The Q-V curves are produced by incrementally increasing the reactive power demand, Q at a candidate bus, and running series of power flows with each change until the power system is not able to meet the demand for the reactive power. Q-V curves have been used by many utilities for determining proximity to voltage collapse so that operators can make good decision to avoid losing system stability (Kundur, 1994; Reis et el, 2009). A typical Q-V curve is shown in Figure 2.7, where the voltages are scheduled rather than reactive loads.

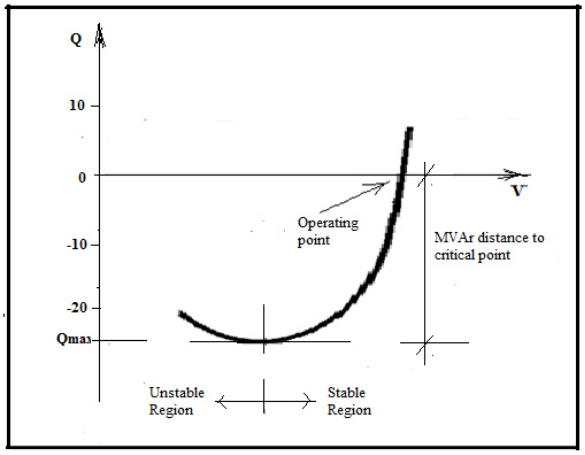

Figure 2.7: Typical *QV* Curve, source: (Mustapha and Murugesan, 2011)

The negative values of reactive supply indicate the increasing reactive load. As shown in the Figure, reactive power margin is measured as a distance between the lowest MVAr point of *QV* curve and voltage axis. Thus reactive power margin indicates how much further the loading on that particular bus can be increased before its loading limit is expired and voltage collapse takes place. The curve can be used as an index for voltage instability. Near the nose of a *QV* curve, sensitivities get very large and then reverse sign. The bottom of *QV* in addition to identifying stability limit, define the minimum reactive power requirement for stable operation (Kundur, 1994).

CHAPTER THREE

METHODOLOGY

3.1 Introduction

To investigate the voltage stability status of the Nairobi Area Distribution Network, a study was conducted to assess the operating voltages at peak loading conditions and to investigate the buses within the network that are susceptible to voltage collapse, the overloaded lines, and the network proximity to voltage stability limit.

The power flow problem for the network configuration was formulated and solution attained by Newton Raphson method. The *VQ* sensitivity and *QV* modal analyses methods discussed in Chapter 2 were employed to investigate the network voltage weak buses and overloaded lines. The buses identified as weak were further investigated by analysing their *PV* and *QV* curve characteristics to determine the network margins to voltage stability limits. The analysis was performed using peak loading data of June, 2012.

3.2 Model of Nairobi Area Power Distribution Network

The network studied is a 59 No. bus system with 66 kV radial distribution lines which originate from four bulk power supply substations at Juju Road-132/66 kV; Ruaraka-132/66 kV; Nairobi North- 220/66 kV; and Embakasi-220/66 kV. Rings of 132 kV and 220 kV transmission lines supply the bulk supply points from six hydroelectric and two geothermal power generation stations operated by KENGEN. The network also has two diesel generator plants at Nairobi South and Embakasi sub-stations, both operated by IPPs, and one hydroelectric power plant at Tanapower station, operated by KENGEN, all injecting power to the 66 kV network. Figure 3.1 below shows the single line diagram of Nairobi Area Power supply Distribution Network.

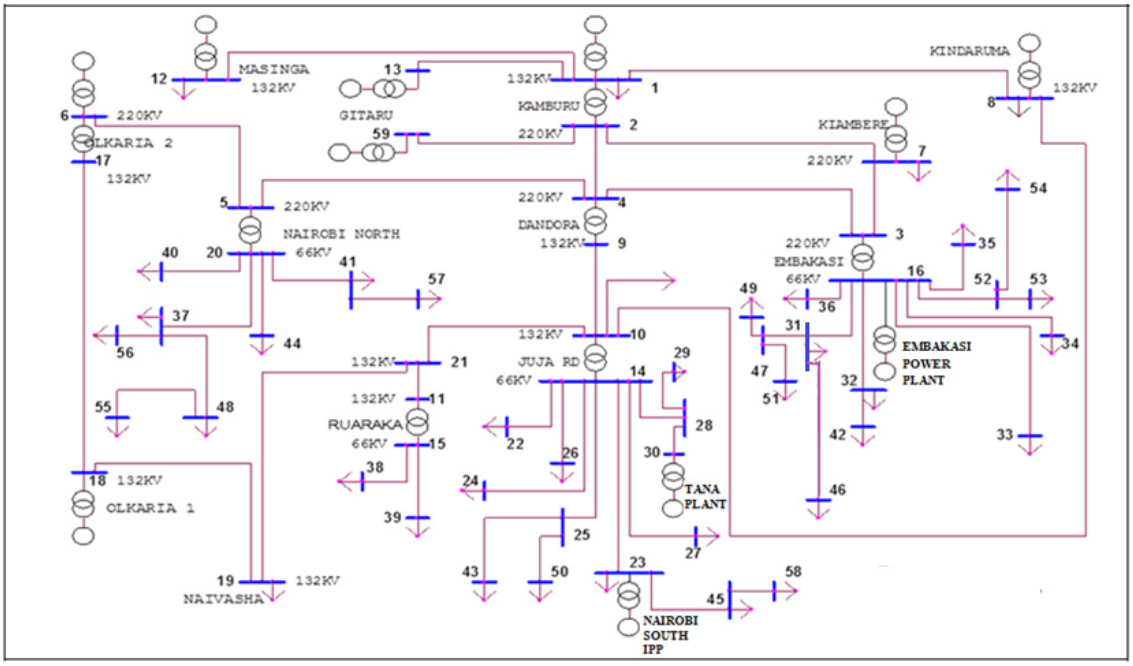

Figure 3.1: Nairobi Area Power Supply Distribution Network as at June, 2012

In this system, Kamburu 132 kV bus was randomly chosen as the slack bus while the generatorbuseswere modeled as standard *PV* buses considering reactive power limits. The nine power generating stations in the network deliver about 725 MW to the network. The load buses were modeled as *PQ* buses. The most loaded buses are: Nairobi south, Nairobi west, Parklands, EPZ, and Thika. However, these buses are located not very farfrom the bulk power sources. All power transformers were modeled as 2-windings transformers with load tap changers. However, in this static analysis, the automatic load tap changers were not considered. The transmission and distribution lines were modeled using the nominal *pi* model. The power flow simulation was conducted using a MATLAB based program discussed in Chapter 2, while PowerFactory DIgSILENT was used for the further analysis, to generate the *PV* and *QV* curves of the identified voltage weak buses. The system load, line and generator data are presented in Appendix A.

3.3 Power Flow Analysis

The power flow problemwas formulated in a MATLAB script file and solution obtained using a MATLAB based computer program for power flow analysis. Several computer programs have been developed for power flow analysis of practical systems. The power flow solution method consists of four function programs, namely: ***lfnewton***, ***lfybus***, ***busout***, *and* ***lineflow*** (Saadat, 1999). These MATLAB functions are used in sequence to compute and display power flow solution in MATLAB workspace. The MATLAB based power flow program in a script file is givenin Appendix B.

The outputs of the power flow solution are: the operating bus voltage and angle profiles, the active and reactive power flows, and the system losses. The voltage criteria for the Kenya's grid code are: +/-6% for the distribution network and +/-10% for transmission networks (Kenya Grid code, 2008). The network base operating voltages were noted and recorded.

For the detailed analysis of the network voltage stability using static tools, the power flow Jacobian matrix was reduced and further analyzed as given in the sections that follow.

3.4 *VQ* Sensitivity

To investigate the *VQ* sensitivity at the load buses, sensitivity factors were computed. Thecoding in MATLAB computed the reduced Jacobian matrix, J_R using the elements of the Jacobian matrix defined in equation (2.14).The sensitivity factors are the diagonal elements of the inverse of J_R as discussed in sub section 2.6.3. Buses with the highest sensitivities were noted and recorded.

3.5 Modal Analysis

To investigate the voltage stability characteristics of the load buses, the coding in MATLAB computed theeigenvalues andthe right and left eigenvectors ofthe J_R computed in section3.4. The minimum eigenvalues were noted and recorded. The smallest sixeigenvalues out of a total of 48 for the case study were analyzed in detail to determine critical modesand the load regions they associate with, as discussed in 2.6.4.

3.5.1 Investigating the Network Voltage Weak Buses

To investigate the voltage weak nodes, the coding in MATLAB computed bus participation factors from the right and left eigenvector matrices, obtained by themodal analysis. The buses with the highest participation factors were noted and recorded.

3.5.2 Investigating Overloaded Branches

The line network areas around the buses identified in sub-section 3.5.1 were investigated to identify the branches which could be overloaded and therefore are prone to voltage collapse. To achieve this, the branch participation factors are calculated. For each mode *i*, it is assumed that thevector of modal reactive power variations, $\Delta Q^{(i)}$ has all elements equal to zero except the *i-th* which equals 1. Based on this assumption, the corresponding bus reactive power variation is the right eigenvector of J_R, as given in expression (2.17). The vector of bus modal voltage variations $\Delta V^{(i)}$, is then calculated by multiplying the $\Delta Q^{(i)}$ by the inverse of the diagonal eigenvalues matrix, as given in expression (2.14) then (2.18). The vector of bus angle variations $\theta^{(i)}$ is computed by multiplying $-J_{P\delta}^{-1}J_{PV}$ by $\Delta V^{(i)}$ as given in expression (2.19). The linear reactive power Q_k, is calculated by computing total differentials, as given in expression (2.21).

A typical example illustrating how the MATLAB based program computes the linear reactive power at bus number 55 in the case study is given as follows:

The vector of modal reactive power variations in mode 30, $\boldsymbol{q}^{(30)}$is computed by MATLAB based program.

The vector of modal voltage variations in mode 30, $\boldsymbol{V}^{(30)}$ is computed by MATLAB based program.

The voltage variation at bus 55 is computed as follows:

$V^{(30)}(45,1) = -0.6640$

The vector of bus angle variations is computed by the program as given in expression (2.19).

Therefore the angle variation at bus 55 is given by:

$\theta_{55} = -J_{Q\delta}J_{QV}(54,45)\times V^{(30)}(45,1)$

$= 0.3242$

The reactive power variations with respect to bus angles are summed for bus 55 as:

$sum(J_{Q\delta}(45,54:end))$

$=-2.7799$

Multiplying this by the vector of bus angle variations:

$sum(J_{Q\delta}(45,54:end))\times\theta_{55}$

$= -0.9014$

The reactive power variations with respect to bus voltages are summed for bus 55 as:

$sum(J_{QV}(45,45:end))$

$= 5.3927$

Multiplyingthis by the vector ofbus voltage variations:

$sum(J_{QV}(45,45:end))\times V^{(30)}(45,1)$

$= -3.5809$

The linear reactive power at bus 55 is computed as:

$Q_{55} = sum(J_{Q\delta}(45,54:end))\times\theta_{55} + sum(J_{QV}(45,45:end))\times V^{(30)}(45,1)$

$= -0.9014 + -3.5809$

$= -4.4823$

Finally, the linear reactive power losses in each branch are calculated as the difference between the sending and receiving end bus linear reactive powers.

The branch participation factors in each mode are calculated as the ratio between linear reactive power losses in a branch to the maximum linear reactive power loss in the mode. Branches with the highest branch participation factors were noted and recorded.

3.6 Investigating Network Proximity to Voltage Collapse

The 59 No. bus Nairobi power supply distribution network was remodeled in PowerFactory DIgSILENT software. This software has the advantage that it utilizes a DIgSILENT Programming Language (DPL) which has an interface for automating tasks in the program and is able to automatically adjust the incremental loading step

variations.The procedure for generating data to produce the *PV* and *QV* curves in PowerFactory DIgSILENT software are presented in the following sub sections.

3.6.1PV Curves

The *PV* curve at a load bus is normally produced by incrementally increasing the active power, *P* and performing series of power flow solutions for the different loading levels, until the maximum power transfer limit is reached as discussed in section 2.6.5. In PowerFactory DIgSILENT software, the candidate bus and the load attached to it are first selected. On execution of the DPL script command (U-P), the software automatically creates the *PV* curves for the selected bus by changing the selected load. In this case study, the process continued until the reactive power limit of the slack bus generator was reached, and the power flow was not able to converge. The *PV* curve is automatically plotted using the calculated values of voltages corresponding to the incremental changes of *P* values at the selected bus.

One set of incremental loading steps automatically generated had typical variation increments of 0.0125, 0.05, 0.1, 0.2, 0.4, 0.8, 1.6, 3.2, and then reduction variations of 1.6, 0.8, 0.4, 0.2, 0.1 and 0.05. The data generated for the *PV* curves for the buses discussed in section 3.4 and sub section 3.5.1 are given in appendix C.

The active power margin for the bus under study was then calculated by subtracting the real power value at the base operating point from the maximum permissible real power, which is at the collapse point, as shown in Figure 2.6, chapter 2. The margin was then expressed as percentage of base active power loading. The calculated MW margins and the percentages were noted and recorded.

3.6.2 QV Curves

The *QV* curve at a load bus is normally produced by incrementally increasing the reactive power, Q and performing series of power flow solutions for the different loading levels, until the power system is not able to meet the demand for the reactive power, as discussed in section 2.6.5. In PowerFactory DIgSILENT software, the candidate bus and the load attached to it are first selected. On execution of the DPL script command (U-Q), it attaches a generator “SC” to the bus and power flow is

performed for voltage set points until the load flow does not converge any longer or the voltage set point is less than zero. A typical voltage set points automatically generated had variations of 0.905, 0.895, 0.885, 0.875, 0.865, 0.855, 0.845, 0.835, 0.825, 0.815, 0.805, 0.795, 0.785, 0.775, 0.765, 0.755, 0.745, 0.735, 0.725, 0.715, 0.705, 0.695, 0.685, 0.675, 0.665, 0.655, 0.645, 0.635, 0.625, 0.615, 0.605, 0.595, 0.585, 0.575, 0.565, 0.555, 0.545, 0.535 and 0.0.525. The data generated for the buses discussed in section 3.4 and sub section 3.5.1 is given in appendix C. The data on voltage set points and reactive power flow of the "SC" are stored in a result folder, from where it can be exported to a work space where the *QV* curve is plotted.

The reactive power margin was calculated by subtracting the reactive power value at base operating point from the maximum permissible reactive power, which is at the base pointof the *QV* curve, as illustrated in Figure 2.7, chapter 2. The calculated reactive power margin was then expressed as a percentage of base operating reactive power. The reactive power margins in MVAr and their percentages were noted and recorded.

CHAPTER FOUR

SIMULATIONS, RESULTS AND DISCUSSIONS

4.1 Introduction

This chapter presents the research results obtainedfrom power flow simulation, modal analysis, sensitivity analysis, and the *PV* and *QV* curves analysis methods of the identified weak buses.

4.2 Load Bus Base Voltages

The power flow converged after 10 iterations with a maximum mismatch of 8.8545e-008. The active and reactive power demands during peak were 725 MW and 237MVAr respectively inclusive of charging power, while the active and reactive power losses in the network were 25.7 MW and 0.9 MVAr respectively.

Table 4.1 gives the load buses with voltages outside the recommended limits, based on the criteria discussed in section 3.3. The base operating voltages for the network load buses are given in Appendix D.

Table 4.1: Load buses operating outside recommended voltage limits

BUS NO	27	29	42	48	49	51	55
VOLTAGE (P.U)	0.91	0.93	0.86	0.93	0.91	0.90	0.92
P (MW)	32.58	37.06	7.13	8.5	12.75	17.25	12.5
Q (MVAr)	10.71	12.17	1.45	2.1	4.45	6.02	2.5
DIST. FROM SOURCE (KM)	28	40	127	31	22	24	46

Bus numbers 27 and 29 supply mostly commercial and industrial load regions. The operating voltage levels at bus numbers 27 and 29 are attributed to motor loads in the industrial regions and enhancement of supply connectivity.

Bus numbers 48 and 55 supply mainly commercial and domestic load regions. Bus number 48 is about 15 km away from bus 55. The operating voltage levels are attributed to feeder losses due to the enhancement of supply connectivity.

Bus number 42 supplies some motor loads at the nearby Magadi Soda Factory and some domestic and commercial loads. The operating voltages levels are attributed to motor loads and losses on long feeder lines.

Bus numbers 49 and 51 supply mainly domestic and commercial load regions. Bus 51 is about 4 km away from bus 49.The operating voltage levels at these buses are attributed to enhancement of supply connectivity.

4.3 *VQ* Sensitivity Analysis

Table 4.2 gives eleven buses with the highest sensitivity factors, while Figure 4.1 is a graphical representation of the same. The sensitivity factors for all the load buses are given in Table E, Appendix E.

Table 4.2: Highest *VQ* sensitivities

Bus No	42	55	27	48	32	57	29
Sensitivity	0.7696	0.4925	0.354	0.3301	0.2832	0.2755	0.2672
Bus No	41	56	49	51			
Sensitivity	0.2238	0.2224	0.189	0.1889			

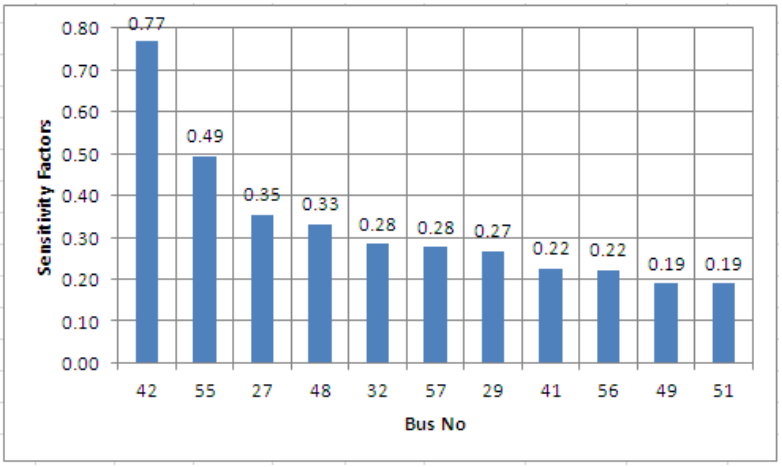

Figure 4.1: The highest *VQ* sensitivity factors

It can be seen from Table 4.2 that buses with high sensitivity factors were also identified with lower base operating voltage levels in section 4.2. As discussed sub-section 2.6.3, these are the buses operating relatively close to the nose of Q-V curve; they experience larger voltage changes for reactive power imports. Hence they are weak buses.

4.4 Modal Analysis

In section 2.6.4, it was discussed that the critical modes in a practical power system with several buses can be identified by computing about 5 to 10 of the smallest eigenvalues. Table 4.3 gives six smallest eigenvalues, out of a total 48 in the network. The 48 eigenvalues of the network are given in Appendix F.

Table 4.3: Six smallest eigenvalues

MODES	30	39	40	32	33	38
EIGENVALUES	0.7	1.1	2.2	2.6	2.9	2.9

As discussed in subsection 2.6.4, the magnitude of the minimum eigenvalue can provide a relative measure of the network proximity to voltage instability, since it becomes zero at bifurcation. Mode 30 is therefore considered critical.

4.4.1 Bus Participation Factors

Table 4.4 gives three buses with highest bus participation factors in mode 30, while Figures 4.2 is the graphical representation of the same. The bus participation factors for all the load buses in mode 30 are given in Appendix G.

Table 4.4: Highest Bus Participation factorsin mode 30

BUS NO	55	48	56
PART. FACTOR	0.2426	0.184	0.1078

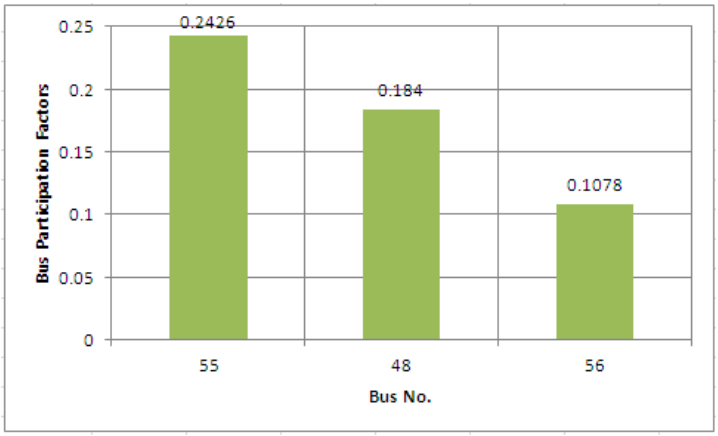

Figure 4.2: Highest bus participation factors in mode 30

Table 4.5 gives two buses with highest bus participation factors in mode 39, while Figure 4.3 is a graphical representation of the same. The bus participation factors for all the buses in modes 39 are given in Appendix G.

Table 4.5: Bus Participation Factors in mode 39

BUS NO	42	32
PART. FACTOR	0.8195	0.1805

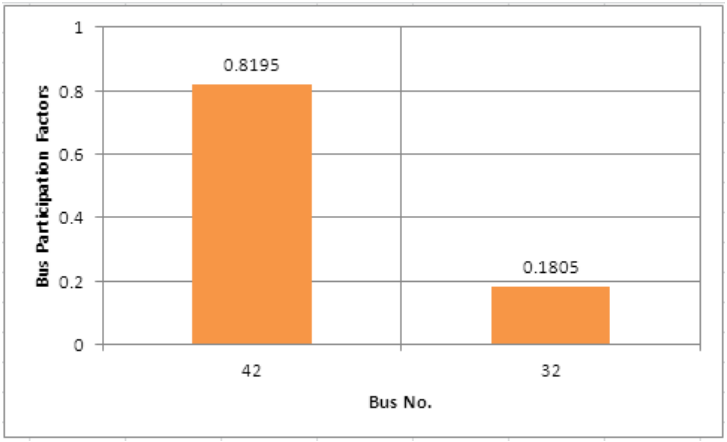

Figure 4.3: Bus participation factors in mode 39

Table 4.6 gives three buses with highest participation factors in mode 40, while Figure 4.4 is a graphical representation of the same. The bus participation factors for all the buses in modes 40 are given in, Appendix G.

Table 4.6: Highest Bus Participation Factors in mode 40

BUS NO.	51	49	47
PART, FACTOR	0.3258	0.3252	0.2322

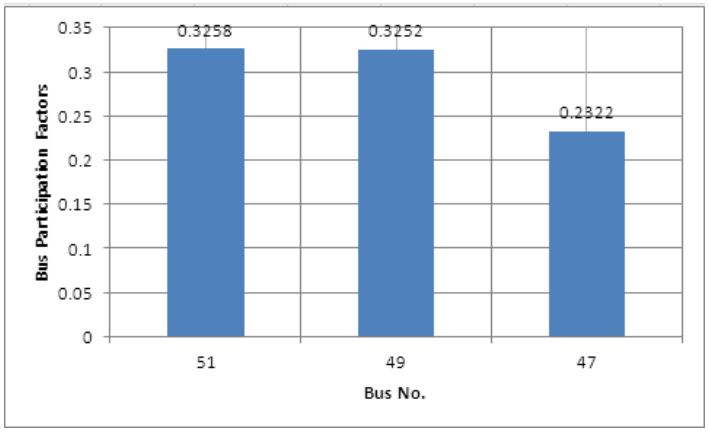

Figure 4.4: Highest bus participation factors to mode 40

Table 4.7 gives three buses with highest bus participation factors in mode 32, while Figure 4.5 is a graphical representation of the same. The bus participation factors for all the buses in modes 32 are given in Appendix G.

Table 4.7: Highest Bus Participation factors in mode 32

BUS NO	27	38	29
PART. FACTORS	0.4229	0.1935	0.1218

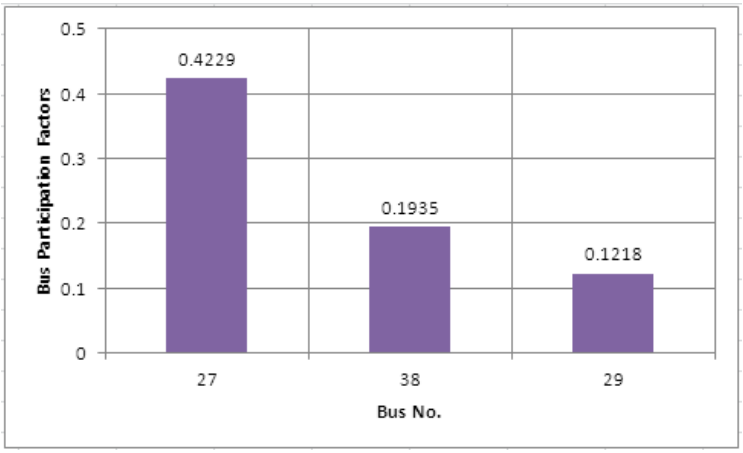

Figure 4.5: Highest bus participation factors in mode 32

Table 4.8 gives one bus with high bus participation factors in mode 33, while Figure 4.6 is a graphical representation of the same. The bus participation factors for all the buses in modes 33 are given in Appendix G.

Table 4.8: Highest Bus Participation Factor in mode 33

BUS NO	27
PART. FACTOR	0.4405

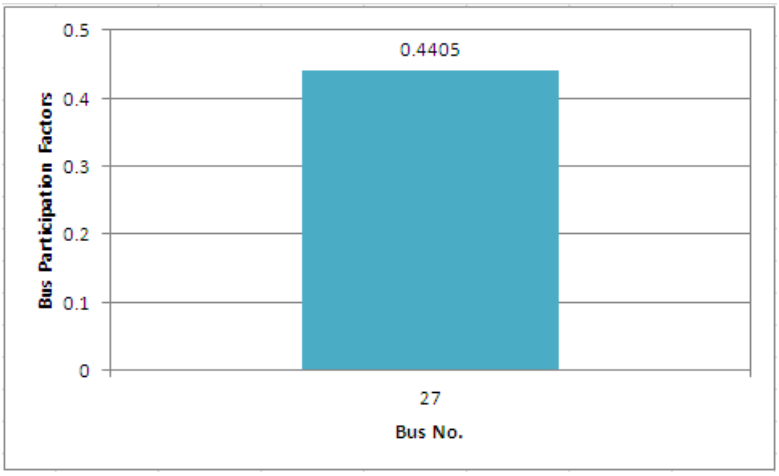

Figure 4.6: Highest bus participation factor to mode 33

Table 4.9 gives one bus with high participation factor in mode 38, while Figure 4.7 is a graphical representation of the same. The bus participation factors for all the buses in modes 38 are given in Appendix G.

Table 4.9: Highest Bus Participation factors in mode 38

BUS	27
PART. FACTOR	0.9973

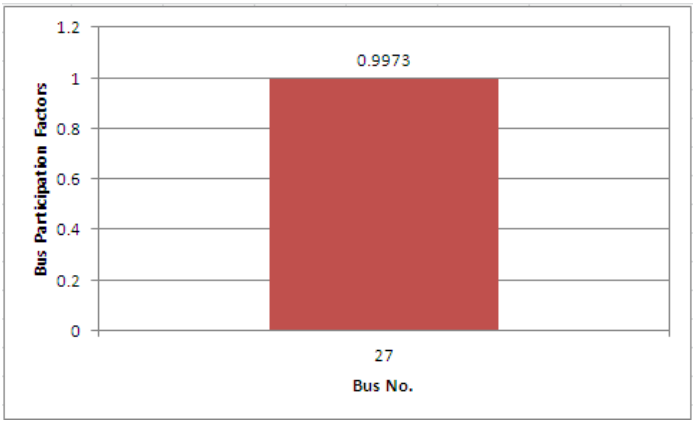

Figure 4.7: Highest Bus Participation Factor in mode 38

From the analysis of the six modes corresponding to the smallest eigenvalues in the network, the following observations are made:

The minimum eigenvalue is 0.7 corresponding to mode 30. This mode is the most critical in the network. For each of the modes discussed, the buses with highest participation factors have been identified as: 55 in mode 30; 27 in modes 32, 33 and 38; bus 42 in mode 39; and bus 51 in mode 40. These buses were also identified with low base operating voltages, and higher sensitivity factors.

For each of the modes investigated, only few buses had high participation factors, while the rest had close to zero factors. This is an indication that the modes are local, and implies the presence of oscillations at these buses.

The results showed that the modes 32, 33 and 38 are associating with same load region (bus number 27). The bus participation factor for bus 27 was highest in mode 38, while

in each of the modes 32 and 33, the factor almost halved, implying of the three modes, bus 27 is weakest in mode 38.

It was observed that the modes 32 and 33 are corresponding to the same modal eigenvalue. As mentioned above, their level of association (participation factor) with bus number 27 is almost the same.

4.4.2 Branch Participation Factors

Table 4.10 gives branches with the highest branch participation factors in mode 30, while Figure 4.8 is a graphical representation of the same.The linear bus reactive powers and the linear branch reactive power losses in mode 30 are given Appendices H and J respectively.

Table 4.10: Highest branch participation factors in mode 30

BRANCH	37-48	48-55	37-56
PART. FACTOR	1	0.5617	0.1129

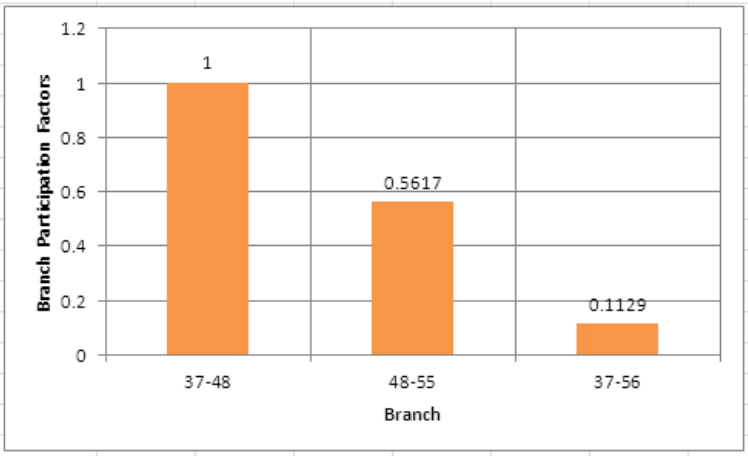

Figure 4.8: The highest branch participation factors to mode 30.

Table 4.11 gives one branch with a participation factor in mode 39, while Figure 4.9 is a graphical representation of the same. The linear bus reactive powers and the linear branch reactive power losses in mode 39 are given in Appendices H and J respectively.

Table 4.11: Branch Participation Factor in mode 39

BRANCH	32 - 42
PART. FACTOR	1

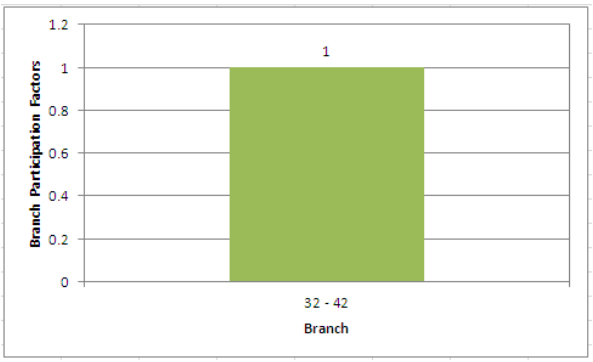

Figure 4.9: The branch participation factor in mode 39

Table 4.12 gives the branches with the highest branch participation factors in mode 40, while Figure 4.10 is a graphical representation of the same. The linear bus reactive powers and the linear branch reactive power losses in mode 40 are given in TablesH3 and J3 respectively in the Appendices H and J respectively.

Table 4.12: Branch Participation Factors in mode 40

BRANCH	31-47	47-51	47-49
PART. FACTOR	1	0.4158	0.3597

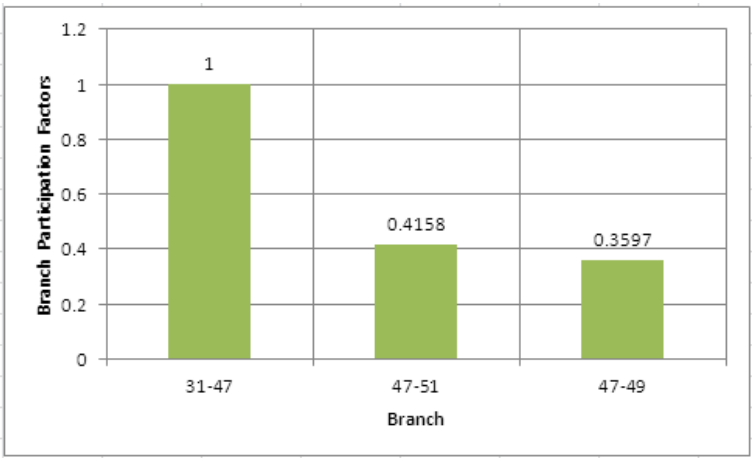

Figure 4.10: The highest branch participation factors in mode 40.

Table 4.13 gives one branch with a participation factor in mode 32, while Figure 4.11 is a graphical representation of the same. The linear bus reactive powers and the linear branch reactive power losses in mode 32 are given in Appendices H and J respectively.

Table 4.13: Branch Participation Factor in mode 32

BRANCH	15 - 38
PART. FACTOR	1

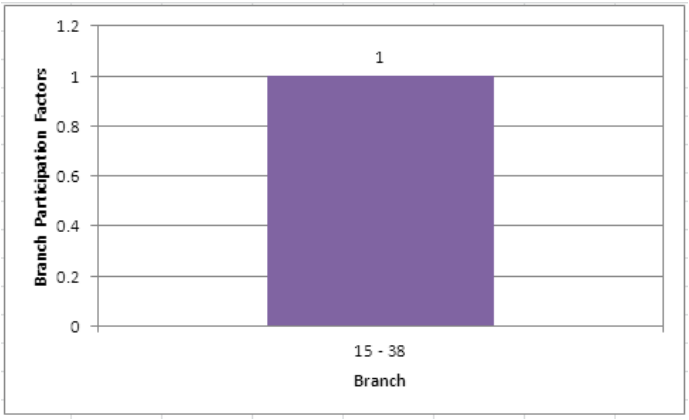

Figure 4.11: The branch participation factor in mode 32.

From the analysis of the six modes to establish the network branches they associate with, the following observations can be made:

Mode 30: the branch 37-48 had the highest branch participation factor. As discussed in 2.6.4 this implies the branch gets overloaded due to high reactive power consumption, which could cause voltage collapse.

Mode 40: the branch 31-47 had the highest branch participation factor implying an overload occurs due to high reactive power consumption in this mode.

For mode 32, only one branch (15-38) associated in the mode.

For mode 39, only one branch (32-42) associated in this mode.

The modes 33 and 38 did not associate with any network branches.

4.5 Active Power Margin

Figures 4.12 - 4.15 gives the *PV* curves plotted for buses identified in section 4.4.1, as having high participation factors.

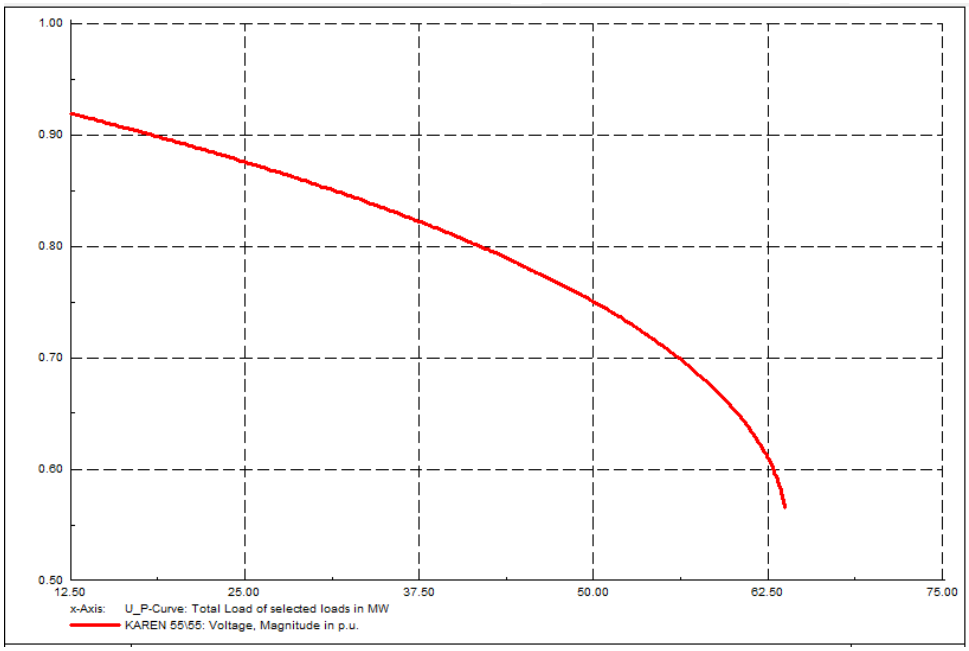

Figure 4.12: PV curve for buss 55

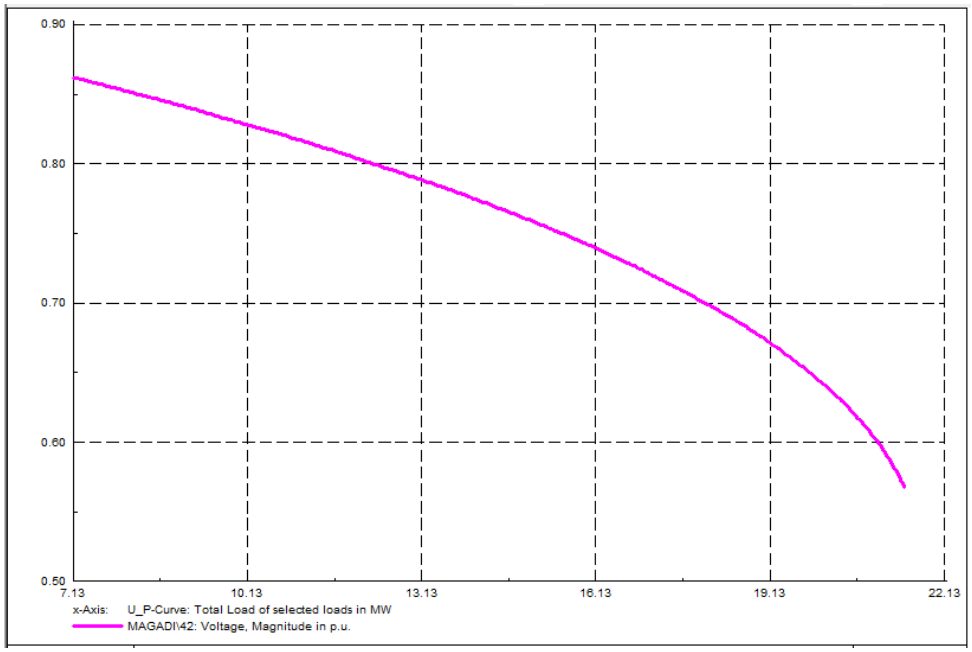

Figure 4.13: PV curve for bus 42

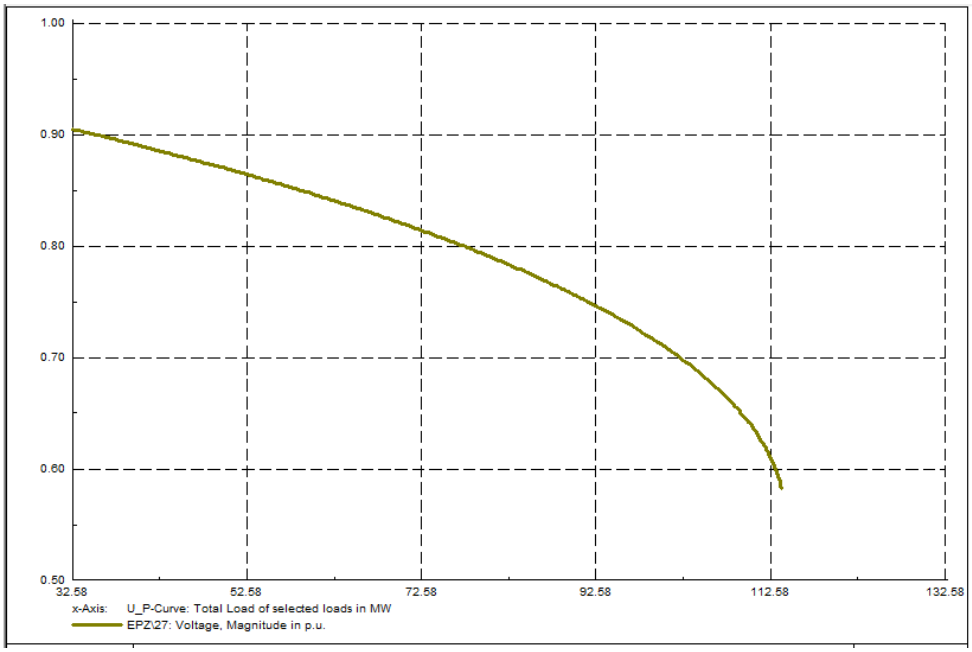

Figure 4.14: PV curve for bus 27

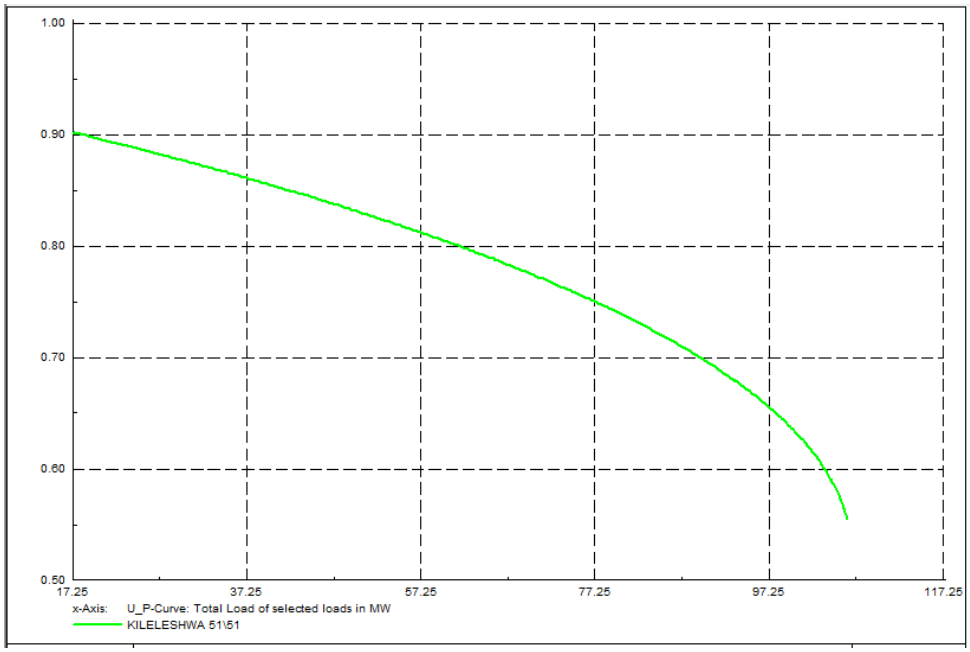

Figure 4.15: PV curve for bus 51

Figure 4.16 gives a *PV* curve showing a comparison of active power loading levels of the four buses identified as critical in their respective modes. It can be seen that bus 42 is the most loaded node of the four.

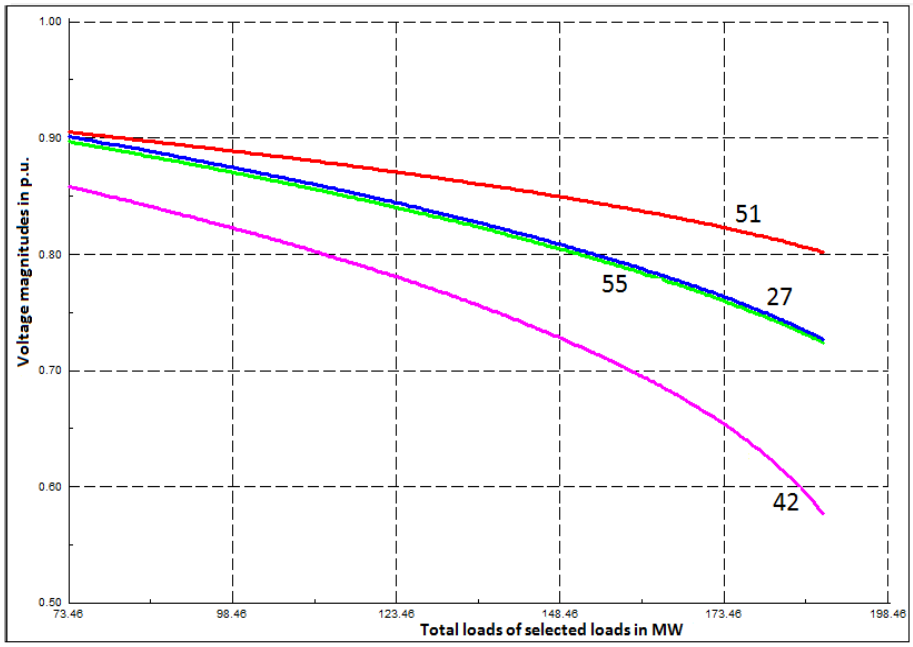

Figure 4.16: PV curve for four most critical buses

Table 4.14 gives the active power margins expressed in MW and also in percentages of the base operating loading levels, calculated for buses whose *PV* curves are produced in Figures 4.12-4.15, while Figure 4.17 is a graphical representation of the same.

Table 4.14: Active Power Margins

BUS NO	42	27	51	55
ACTIVE POWER MARGIN (MW)	14.3	81.3	64	51.2
ACTIVE POWER MARGIN (%)	201	250	371	410

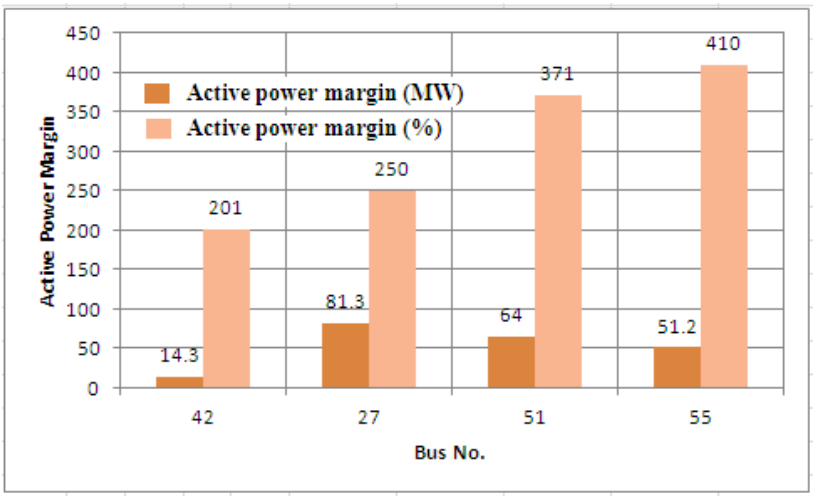

Figure 4.17: Active Power margins in MW and percentage

Bus number 42 has the least percentage active power margin to stability limit. As discussed in sub-section 2.6.5, this implies the operation point is closest to maximum active power transfer point.

4.6 Reactive Power Margin

Figures 4.18-4.21 gives the *QV* curves plotted for the buses discussed in section 4.4.1.

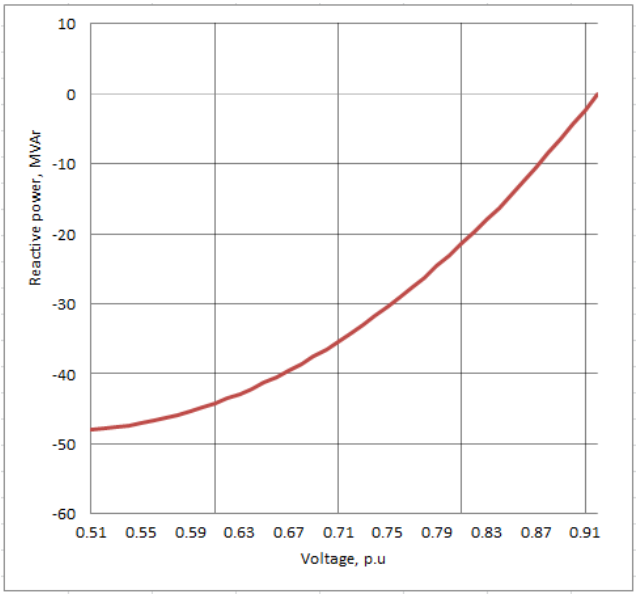

Figure 4.18: *QV* curve for bus 55

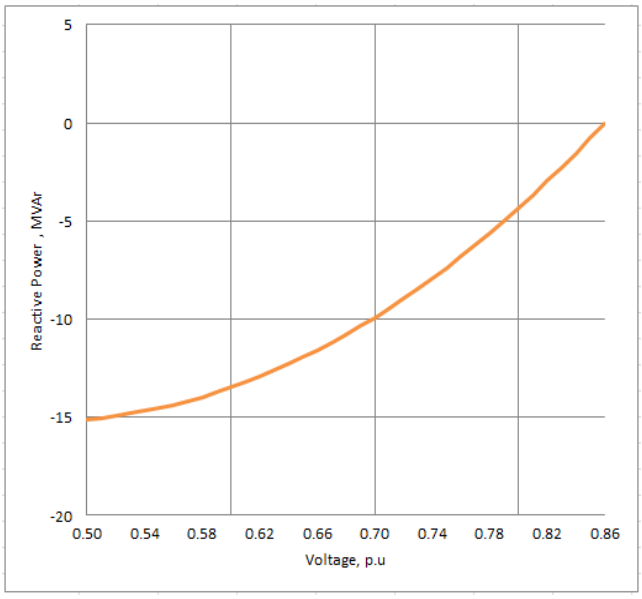

Figure 4.19: *QV* curve for bus 42

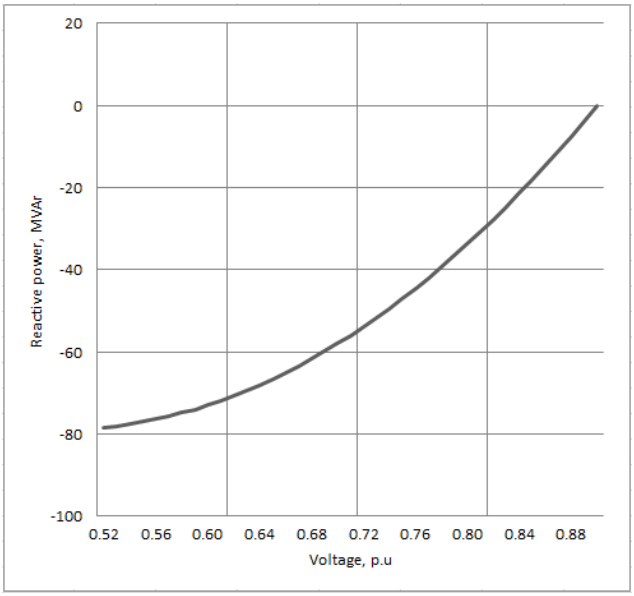

Figure 4.20: *QV* curve for bus 27

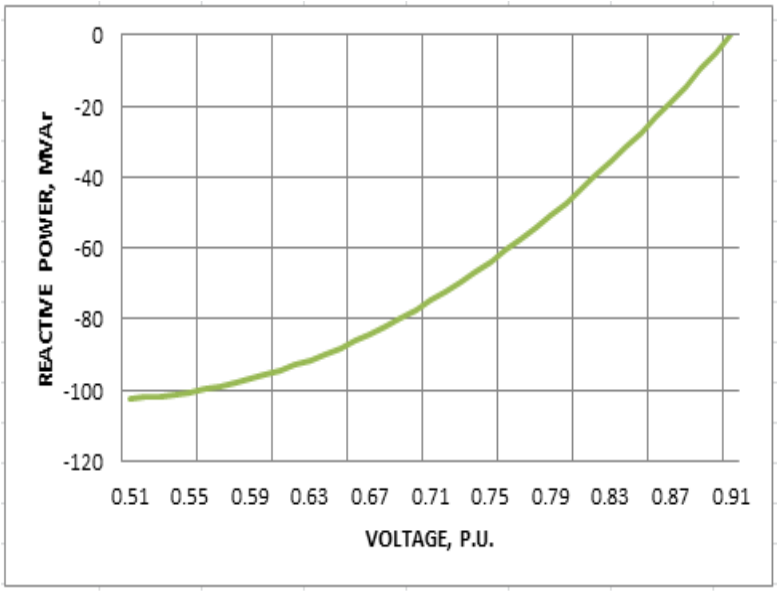

Figure 4.21: *QV* curve for bus 51

Figure 4.22 gives a QV curve, showing comparison of the reactive power loading levels of the four buses identified as critical in their respective critical modes. It can be seen that bus 42 is the most loaded node of the four.

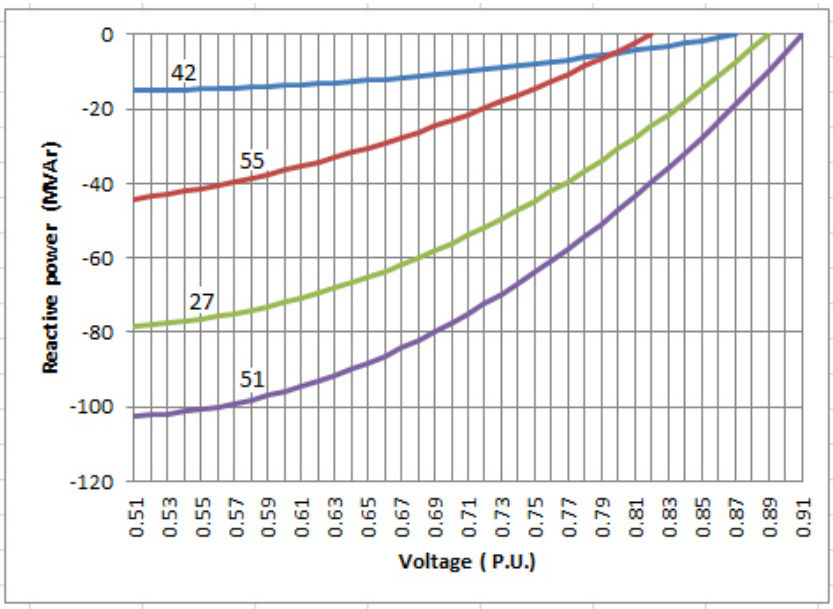

Figure 4.22: QV curve for four most critical buses

Table 4.15 gives the reactive power margins expressed in MVArs and also in percentages of the base operating loadings, calculated for the buses whose *QV* curves are shown in Figures 4.17-4.20, while Figure 4.23 is a graphical representation of the same.

Table 4.15: Reactive Power Margins

BUS NO	27	42	51	55
REACTIVE POWER MARGIN (MVAr)	78.4	15	96.4	48
REACTIVE POWER MARGIN (%)	732	1034	1603	1920

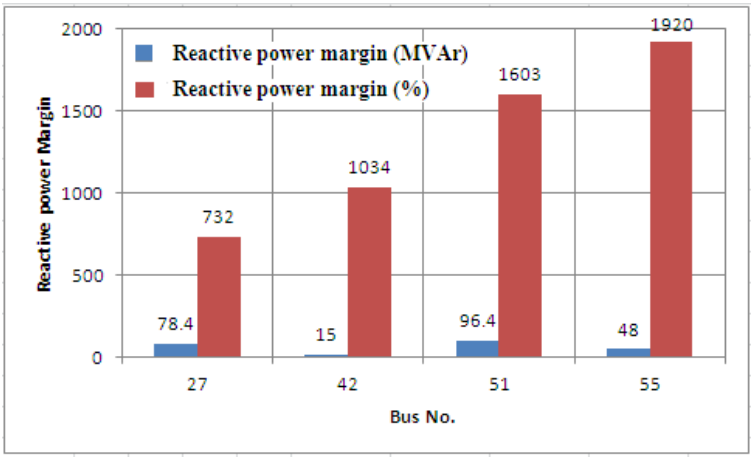

Figure 4.23: Reactive power margins in MVAr and Percentage

Bus number 27 has the least reactive power margin to stability limit. As discussed in sub-section 2.6.5, this implies the operation point is closer to the stability limit, which also explains the high sensitivity factor exhibited at the bus, in section 4.3.

4.7 Remedial Measures

The presentations in sections 4.3 through to 4.6 identified the buses operating relatively closer to voltage stability limit. Mitigation measures are required to prevent the network slide to voltage collapse.

The buses: 27 (EPZ), 42 (MAGADI), 51(KILELESHWA) and 55 (KAREN) were identified as the voltage weak buses in their respective modes of associations, where the voltage collapse incident in the network could occur. The recommended remedy is to place of adequate reactive power support at these buses to enhance their voltage stability margins. As discussed in section 2.5, the reactive support can be achieved by constructing generating stations closer to the load centers, synchronous condensers, SVCs and Shunt capacitors. At bus 42 where space is not a constraint and reactive power demand have had to be transported over long feeder lines, it is recommended that a generation plant be constructed close to the bus, to provide reactive power support there. Bus 55 is located close to Ngong wind power station, the recommendation is to develop the 66 kV infra-structures all the way from the wind power station and inject

wind power to the bus at 66 kV. Static VAr compensating (SVC) devices is recommended at each of the buses 51 and 27.

The branches 37-48 (LIMURU-KIKUYU), 31-47 (NAIROBI WEST-NGONG ROAD JUNCTION), 32-42 (MATASIA-MAGADI) and 15-38 (RUARAKA BULK STATION-RUARAKA 66 KV) were identified as most overloaded at peak conditions. The 66 kV distribution network is constructed in ACSR conductors of size 150mm^2, while the Ruaraka link is short length of copper tubes, 4 mm thick, outside diameter-76mm.It is recommended to re-inforce these lines sections with the emphasis being to provide additional feeder circuits or re-conductor the feeders with larger cross sectional area size conductors. However, it is noted that re-conductoring alone does not reduce the network demand for reactive power since the reactive power consumed by the network is proportional to the square of the line current. Where this is the option, it is recommended that the implementation is done in conjunction with series compensation.

CHAPTER FIVE
CONCLUSIONS AND RECOMMENDATIONS

5.1 Conclusions

The study has assessed the voltage stability status of Nairobi area distribution network using *VQ* sensitivity, *QV* modal and *PV* and *QV* curves analyses methods. The load buses base operating voltages were obtained from the power flow solution of the network.

Modal analysis was used to identify the voltage weak buses, where the voltage instability problems could occur. These buses are: 27 (EPZ), 42 (Magadi), 51 (Kileleshwa) and 55 (Karen). The branches which consume most reactive power, and therefore are overloaded were identified as: 37-48 (Limuru-Kikuyu), 31-47 (Nairobi West-Ngong Road junction), 15-38 (Ruaraka bulk power station–Ruaraka), and 32-42 (Matasia-Magadi).

Modal analysis further gave indications that the network operation is relatively close to voltage in stability as given by the magnitude of the smallest eigenvalue (0.7). However since all the eigenvalues are positive, this implies the operation has not reached collapse point.

Sensitivity analysis identified the voltage weak buses in the network, but without indicating the modes they associate with. The buses identified as voltage weak by the modal analysis, were found to have high sensitivity factors, confirming they are weak buses. Sensitivity factors for all the network load buses were positive. This is an indication that the network operation has not reached voltage collapse point, which corroborates the findings by the modal analysis method.

The active and reactive power margins for the identified buses were calculated from the *PV* and *QV* curves. The margins were then expressed as percentages of the base loading conditions of the respective buses. Comparison of these percentages showed that bus numbers 42 and 27 had the least active and reactive power margins respectively to the

voltage collapse point. This suggests that bus 42 is most critical with respect to active power transfer, whereas bus 27 is most critical with respect to reactive power transfer.

The study provided an opportunity for a better understanding of how the sensitivity and modal analyses methods and the PV and QV curve methods can be applied to assess the voltage stability status of a distribution network. By application of these methodologies, all the objectives of this study were met. Finally remedial measures are proposed, which if implemented may prevent the network slide to voltage collapse as the network topology and loadingschanges.

5.2 Recommendations

The Kenyan power system is still at its infancy and the loading and topology of the distribution network is known to change relatively fast. It is recommended that voltage stability analysis be conducted at regular time intervals to determine the stability status of the network.

The study identified presence of localized mode oscillations at the voltage weak buses. Further studies recommended to identify the machines involved in each case and the actions to reduce them.

A number of remedial measures have been given in section 4.7 to counter voltage instability. Further analysis is recommended on the application of each of the measures to the distribution network. This will provide answer to questions about the investment and the required device sizes.

REFERENCES

Ajjarapu V (2006). "*Computational Techniques for Voltage Stability assessment and Control*" Springer, 2006

Althowibi, F.A. Mustafa, M.W. (2010). "Maximum power system Loadability to detect Voltage Collapse" *Proc. Power Engineering and Optimization Conference (PEOCO2010)*,

Arrillaga, J., Arnold, C.P (1994) *Computer Analysis of Power Systems*. New York, John Willey & Sons,

Chakrabarti A.and Halder, S. (2012). *Power System Analysis Operation and Control*. New Dehli, PHI.

Cutsen, T. and V., Vournas C. (2008). *Voltage Stability of Electric Power Systems*. New York, Springer.

Das D.(2006). *Electrical Power Systems.* New Dehli, New Age International (P) Limited, Publishers.

Das J. C. (2001). *Power System Analysis*. NewYork, Marcel Dekker Inc.

Ellithi, K., Gastli, A., Al-Alawi, Al-Hinai, S. A. and Al-Abri, Z. (2000). "Voltage Stability Analysis of Muscat Power system during summer weather conditions" *Proc. ASEE conference*, 5, 35-45.

Enemouh, F.O., J Onuegbu,.C. and Anazia E.A (2013). Modal based analysis and evaluation of voltage stability of bulk power systems" *International Journal of Engineering and Development*, 6(12), 71-79,

Energy Regulatory Commission,(2008). Kenya Electricity Grid Code. Nairobi. ERC

Gajjor, G. and Samon, S.A. (2012). "Power System Oscillation modes identifications: Guidelines for applying TLS-ESPRIT Method." *Proc. 17th National Power Systems conference,* 12-14

Gunner, S. and Bilir, B. (2010). Analysis of Transmission Congestion using Power flow solutions" Proc. 5th IASME/WSEAS International conference on energy and environment, Feb. 23-25,

Hasani, M. and Parniani ,M. (2005). Method of Combined Static and Dynamic Analysis of Voltage collapse in Voltage stability Assessment'' *Proc. Transmission and Distribution Conference and Exhibition: Asia and Pacific, IEEE/PES* pp.1-6.

Khami, M.J., Atiyahsity, B.T., Ashem, K.M. (2010) "Computer Aided Stability Analysis in Power System'' *Journal of Thi-Qar University*, (5), special number.

Kothari, D.P. Nagrath I.J. (2006). *Power System Engineering''* New Dehli, Tata McGraw Hill, 2008

Kundur P. (1994). *Power System Stability and Control* New York, McGraw Hill,

Larki, F. Joorabian, M. H. Kelk, M and Pishvaei M. (2010). "Voltage Stability Evaluation of the Khuzestan Power System, Iran Using CPF Method and Modal analysis" *Proc. Power and Engineering Conference (APPEEC),pp.5183-5187.*

Ministry of Energy publication, Kenya, (2011), Least Cost Power Development Plan (LCPDP), Nairobi. Government press.

Morison, K. ; Hamadani, Wang , H. L. (2006). Load Modeling for Voltage Stability Studies" *Power Systems conference and exposition (PSCE), pp.564-568.*

Mustapha, P. and Murugesan, G. (2011). Transmission Line stability Improvement using TCSC. *InternationalJournal of Engineering Science and Technology*, 3, (2), 163-173,

Reis, C A. Andrade, F.P.M. Barbosa "Methods of Preventing Voltage Collapse" Proc. International Conference on Electrical and Electronic Engineering, 2009

Saadat H. (2008). *Power system analysis*. New York. McGraw Hill, 1999

Zerwa, M. (2010). *Voltage Stability Assessment of Swiss Power Transmission System.* unpublished *M*Sc thesis. Swiss Federal Institute of Technology (ETH), Zurich

APPENDICES

APPENDIX A

SYSTEM DATA

Table A1: Load Data

BUS NO,	1	7	8	12	10	19	22
BUS NAME	KAMB 132KV	KIAM 220KV	KINDA 132KV	MAS 132KV	JUJ RD 132kV	NAIV 132kV	BABA DOGO
PL (MW)	14.02	15	4	36.25	3	23.25	22.39
QL (MVAr)	4.89	5.23	1.5	12.29	0	8.1	7.36
BUS NO,	23	24	26	27	29	31	32
BUS NAME	NAIR SOUTH	EMCO	PARK LAND	EPZ	THIK	NAIR WEST	MAT
PL (MW)	59.52	25.25	44.8	32.58	37.06	34.59	9.375
QL (MVAr)	19.56	8.29	14.72	10.71	12.17	12.06	3.26
BUS NO,	33	34	35	36	37	38	39
BUS NAME	ATHI RIVER	NEW AIRPRT	NSSF	MOM RD	LIM	RUI STE MIL	RUAR
PL (MW)	34.21	14.66	30.14	21.99	13.25	8.71	23.36
QL (MVAr)	11.21	4.82	9.9	7.23	4.71	3.07	8.14
BUS NO,	40	41	42	43	44	45	46
BUS NAME	CIA	KIT	MAG	JEEV	WEST LAND	KPC NAIR	CATH
PL (MW)	12.23	15.75	7.13	18.5	15.75	1.3	14.06
QL (MVAr)	3.19	5.49	1.45	6.45	5.49	0.66	4.9
BUS NO,	48	49	50	51	53	54	55
BUS NAME	KIKU	NGON RD	KIMAT	KILEL	NEW IND	FIRE STONE	KAR
PL (MW)	8.5	12.75	10.73	17.25	26.93	2.61	12.5
QL (MVAr)	2.1	4.45	3.74	6.02	9.39	1.26	2.5
BUS NO,	56	57	58				
BUS NAME	KPC NGEM	GIGIRI W/W	MORR & CO				
PL (MW)	2.16	3.4	1				

QL (MVAr)	0.5	1.74	0.22

Table A2: Generator Data

BUS NO.	1	6	7	8	12	13	16	18	23	30	59
BUS NAME	KAM	OLK II	KIA	KIN	MAS	GITARU 132KV	EMB	OLK I	NAI SOUTH	TAN	GITARU 220KV
V (P.U)	1.09	1.052	1.095	1.094	1.093	1.08	1	1.031	1.01	1.015	1.042
Pg (MW)	0	89	130	45	28	73	60	44	100.5	20	60
Qmax (MVAr)	0	69	40	8	20	80	19.2	15	33	6.6	20
Qmin (MVAr)	0	-33	-16	-1	-16	-20	0	0	0	0	-10

Table A3: Line Data

(Base MVA=100;Base kV=66, 132 and 220)

FROM BUS	1	1	1	2	2	3	3	4	5
TO BUS	8	12	13	4	7	4	7	5	6
R (P.U)	0.019	0.0076	0.004	0.0081	0.0074	0.0013	0.0232	0.0009	0.006
X (P.U)	0.0443	0.0456	0.0093	0.0484	0.0302	0.0054	0.1357	0.0056	0.0377
1/2Bc	0.0086	0.0052	0.003	0.1389	0.0459	0.0164	0.1939	0.0159	0.0079
FROM BUS	8	9	10	21	11	18	14	14	14
TO BUS	10	10	21	19	21	19	22	23	24
R (P.U)	0.1229	0.0004	0.0029	0.0414	0.0009	0.0096	0.0225	0.0084	0.0059
X (P.U)	0.2868	0.0024	0.006	0.0863	0.0018	0.0572	0.0434	0.0163	0.011
1/2Bc	0.0558	0.0009	0.0012	0.0323	0.0007	0.0106	0.0006	0.0002	0.0001
FROM BUS	14	14	14	14	15	15	16	16	16
TO BUS	25	26	27	28	38	39	31	32	33
R (P.U)	0.0128	0.0372	0.168	0.0757	0.0492	0.0011	0.0247	0.1395	0.0396
X (P.U)	0.0247	0.1567	0.2887	0.1522	0.0952	0.002	0.0478	0.2644	0.0766
1/2Bc	0.0003	0.0007	0.003	0.0019	0.0012	0.0001	0.0006	0.0032	0.0007
FROM BUS	16	16	16	16	17	20	20	20	20
TO BUS	52	34	35	36	18	37	40	41	44
R (P.U)	0.0159	0.012	0.0341	0.0011	0.0012	0.02952	0.0258	0.0572	0.0396
X (P.U)	0.03075	0.0219	0.0621	0.002	0.0081	0.05712	0.0499	0.1106	0.0766
1/2Bc	0.0004	0.0004	0.0007	0.0001	0.0013	0.0007	0.0006	0.0014	0.0009
FROM BUS	23	25	25	28	28	31	31	32	37
TO BUS	45	43	50	29	30	46	47	42	48
R (P.U)	0.0071	0.0128	0.0197	0.0787	0.0877	0.0087	0.0323	0.2214	0.0693
X (P.U)	0.0152	0.02475	0.0381	0.1522	0.1691	0.0093	0.0624	0.4284	0.134
1/2Bc	0.00022	0.00035	0.0005	0.0019	0.0021	0.0001	0.0008	0.0054	0.0017
FROM BUS	37	41	45	47	47	48	52	52	59
TO BUS	56	57	58	49	51	55	53	54	2
R (P.U)	0.0258	0.0258	0.0083	0.0323	0.0323	0.0693	0.0237	0.0056	0.004
X (P.U)	0.0499	0.0499	0.016	0.0634	0.0624	0.134	0.04585	0.01085	0.0093
1/2Bc	0.0006	0.0006	0.0002	0.0008	0.0008	0.0017	0.0005	0.0001	0.003

APPENDIX B

POWER-FLOW PROGRAM

```
basemva=100;accuracy=0.0001;acc=1.8;maxiter=100;
% Nairobi Area Power Distribution Network
% Bus data [ ]
% Line data [  ]
%Load flow by newton Raphson method
Lfybus
Lfnewton
Busout
Lineflow

 % CREATING IDEALISED JACOBIAN TO OBTAIN J1 J2 J3 AND J4

A;
J1=zeros(58);
m=1;
fori=1:58
    n=1;
for j=1:58
J1(m,n)=A(i,j);
        n=n+1;
end
    m=m+1;
end
J2=zeros(58,48);
m=1;
fori=1:58
    n=1;
for j=59:106
J2(m,n)=A(i,j);
        n=n+1;
end
    m=m+1;
end
J3=zeros(48,58);
m=1;
fori=59:106
    n=1;
for j=1:58
J3(m,n)=A(i,j);
        n=n+1;
end
    m=m+1;
end
J4=zeros(48,48);
m=1;
fori=59:106
    n=1;
for j=59:106
```

```
J4(m,n)=A(i,j);
        n=n+1;
end
    m=m+1;
end

J1
J2
J3
J4

%REDUCED JACOBIAN MATRIX
JR=J4-J3/J1*J2;
JR

%SENSITIVITY ANALYSIS
%VQ REDUCED JACOBIAN=inv(JR);
SENSITIVITY=diag(inv(JR));
SENSITIVITY
%MODAL ANALYSIS
%RIGHT EIGENVECTOR & DIAGONAL MATRIX OF REDUCED JACOBIAN MATRIX
[V,D]=eig(JR);
Eigenvalues=diag(D);
Eigenvalues
T=normc(V)

%LEFT EIGENVECTORS OF REDUCED JACOBIAN MATRIX
W=normr(V')

%COMPUTING BUS PARTICIPATION FOR MODE- 30
PK30=diag(T(1:end,30)*W(30,1:end));
PK30
%COMPUTING BUS PARTICIPATION FOR MODE 40
PK40=diag(T(1:end,40)*W(40,1:end));
PK40
%COMPUTING BUS PARTICIPATION FACTORS FOR MODE 39
PK39=diag(T(1:end,39)*W(39,1:end));
PK39
%COMPUTING PARTICIPATION FACTORS FOR MODE-38
PK38=diag(T(1:end,38)*W(38,1:end));
PK38
% Computing Branch Participation Factors for mode 30;
%Vector of modal reactive power variations for mode-30;
q30=T(1:end,30);
q30
%vector of modal voltage variation for mode-30;
v30=(D(30,30))\q30;
v30
%Vector of modal angle variations for mode-30;
B=-J1\J2;
d5=B(4,4)*v30(4,1);
d5
d21=B(20,13)*v30(13,1);
d21
d37=B(36,27)*v30(27,1);
d37
```

```
d40=B(39,30)*v30(30,1);
d40
d41=B(40,31)*v30(31,1);
d41
d44=B(43,34)*v30(34,1);
d44
d48=B(47,38)*v30(38,1);
d48
d55=B(54,45)*v30(45,1);
d55
d56=B(55,46)*v30(46,1);
d56
d57=B(56,47)*v30(47,1);
d57

%Computing Linear Bus Reactive Power in mode 30
G5=sum(J3(4,4:end))*d5;
G21=sum(J3(13,20:end))*d21;
G37=sum(J3(27,36:end))*d37;
G40=sum(J3(30,39:end))*d40;
G41=sum(J3(31,40:end))*d41;
G44=sum(J3(34,43:end))*d44;
G48=sum(J3(38,47:end))*d48;
G55=sum(J3(45,54:end))*d55;
G56=sum(J3(46,55:end))*d56;
G57=sum(J3(47,56:end))*d57;
F5=sum(J4(4,4:end))*v30(4,1);
F21=sum(J4(13,13:end))*v30(13,1);
F37=sum(J4(27,27:end))*v30(27,1);
F40=sum(J4(30,30:end))*v30(30,1);
F41=sum(J4(31,31:end))*v30(31,1);
F44=sum(J4(34,34:end))*v30(34,1);
F48=sum(J4(38,38:end))*v30(38,1);
F55=sum(J4(45,45:end))*v30(45,1);
F56=sum(J4(46,46:end))*v30(46,1);
F57=sum(J4(47,47:end))*v30(47,1);
Q5=G5+F5
Q21=G21+F21
Q37=G37+F37
Q40=G40+F40
Q41=G41+F41
Q44=G44+F44
Q48=G48+F48
Q55=G55+F55
Q56=G56+F56
Q57=G57+F57

% Computing Branch Participation Factors for mode 39;
%Vector of modal reactive power variations for mode 39;
q39=T(1:end,39);
q39;
%vector of modal voltage variation for mode 39;
v39=(D(42,42))\q39;
```

```
v39;
%Vector of modal angle variations for mode 39;
B=-J1\J2;
d32=B(31,22)*v39(22,1);
d32;
d42=B(41,32)*v39(32,1);
d42;
%Computing Linear Bus Reactive Power FOR BUS 39
G32=sum(J3(22,31:end))*d32;
G42=sum(J3(35,41:end))*d42;
F32=sum(J4(22,22:end))*v39(22,1);
F42=sum(J4(32,32:end))*v39(32,1);
Q32=G32+F32
Q42=G42+F42

% Computing Branch Participation Factors for mode 40;
%Vector of modal reactive power variations for mode-40;
q40=T(1:end,40);
q40;
%vector of modal voltage variation for mode 40;
v40=(D(40,40))\q40;
v40;
%Vector of modal angle variations for mode 40;
B=-J1\J2;
d51=B(50,41)*v40(41,1);
d51;
d49=B(48,39)*v40(39,1);
d49;
d47=B(46,37)*v40(37,1);
d47;
d46=B(45,36)*v40(36,1);
d46;
d31=B(30,21)*v40(21,1);
d31;
%Computing Linear Bus Reactive Power in mode 40;
G51=sum(J3(41,50:end))*d51;
G49=sum(J3(39,48:end))*d49;
G47=sum(J3(37,46:end))*d47;
G46=sum(J3(36,45:end))*d46;
G31=sum(J3(21,30:end))*d31;
F51=sum(J4(41,41:end))*v40(41,1);
F49=sum(J4(39,39:end))*v40(39,1);
F47=sum(J4(37,37:end))*v40(37,1);
F46=sum(J4(36,36:end))*v40(36,1);
F31=sum(J4(21,21:end))*v40(21,1);
Q51=G51+F51
Q49=G49+F49
Q47=G47+F47
Q46=G46+F46
Q31=G31+F31

% Computing Branch Participation Factors for mode 38;
%Vector of modal reactive power variations for mode 38;
```

```
q38=T(1:end,38);
q38;
%vector of modal voltage variation for mode 38;
v38=(D(38,38))\q38;
v38;
%Vector of modal angle variations for mode 38;
B=-J1\J2;
d14=B(13,8)*v38(8,1);
d14;
d27=B(26,18)*v38(18,1);
d27;
d38=B(37,28)*v38(28,1);
d38;
d29=B(28,20)*v38(20,1);
d29;
d15=B(14,9)*v38(9,1);
d15;
d39=B(38,29)*v38(29,1);
d39;
d11=B(10,7)*v38(7,1);
d11;
d21=B(20,13)*v38(13,1);
d21;
d26=B(25,17)*v38(17,1);
d26;
d28=B(27,19)*v38(19,1);
d28;

%Computing Linear Bus Reactive Power in mode 38;
G14=sum(J3(8,7:end))*d14;
G27=sum(J3(18,26:end))*d27;
G38=sum(J3(28,37:end))*d38;
G29=sum(J3(20,28:end))*d29;
G15=sum(J3(9,14:end))*d15;
G39=sum(J3(29,38:end))*d39;
G11=sum(J3(7,10:end))*d11;
G21=sum(J3(13,20:end))*d21;
G26=sum(J3(17,25:end))*d26;
G28=sum(J3(19,27:end))*d28;

F14=sum(J4(8,8:end))*v38(8,1);
F27=sum(J4(18,18:end))*v38(18,1);
F38=sum(J4(28,28:end))*v38(28,1);
F29=sum(J4(20,20:end))*v38(20,1);
F15=sum(J4(9,9:end))*v38(9,1);
F39=sum(J4(29,29:end))*v38(29,1);
F11=sum(J4(7,7:end))*v38(7,1);
F21=sum(J4(13,13:end))*v38(13,1);
F26=sum(J4(17,17:end))*v38(17,1);
F28=sum(J4(19,19:end))*v38(19,1);
```

```
Q14=G14+F14
Q27=G27+F27
Q38=G38+F38
Q29=G29+F29
Q15=G15+F15
Q39=G39+F39
Q11=G11+F11
Q21=G21+F21
Q26=G26+F26
Q28=G28+F28
```

APPENDIX C

C1. THE INCREMENTAL LOAD VARIATIONS FOR P-V CURVES GENERATED IN POWERFACTORY DIGSILENT

Table C1.1: Bus 55 (Karen)

Active power MW	voltage p.u	Active power MW	voltage p.u	Active power MW	voltage p.u
12.5	0.91934	41.2875	0.80322	62.0875	0.619647
12.5125	0.9193	42.8875	0.794522	62.2875	0.615288
12.525	0.919261	44.4875	0.785425	62.4875	0.610641
12.5375	0.919221	46.0875	0.775879	62.6875	0.605614
12.5625	0.919142	47.6875	0.765823	62.8875	0.600157
12.5875	0.919062	49.2875	0.755178	63.0875	0.594111
12.6375	0.918904	50.8875	0.743847	63.1875	0.590799
12.6875	0.918745	51.6875	0.737885	63.2875	0.58724
12.7875	0.918427	52.4875	0.731699	63.3875	0.583372
12.8875	0.918108	53.2875	0.725265	63.4875	0.579098
13.0875	0.917469	54.0875	0.718556	63.5875	0.574263
13.2875	0.916829	54.8875	0.711536	63.6375	0.571556
13.6875	0.915544	55.6875	0.704164	63.6875	0.56854
14.0875	0.914251	56.4875	0.696372	63.7375	0.565171
14.8875	0.911645	57.2875	0.688117		
15.6875	0.90901	58.0875	0.679299		
17.2875	0.903652	58.4875	0.674643		
18.8875	0.898169	58.8875	0.669798		
22.0875	0.886806	59.2875	0.66474		
25.2875	0.874863	59.6875	0.659442		
28.4875	0.862269	60.0875	0.653867		
31.6875	0.848936	60.4875	0.647972		
33.2875	0.841958	60.8875	0.641698		
34.8875	0.834752	61.2875	0.634968		
38.0875	0.819576	61.6875	0.627671		
39.6875	0.81156	61.8875	0.623762		

Table C 1.2: Bus 42 (Magadi)

Active power MW	voltage p.u	Active power MW	voltage p.u
7.13	0.862019	17.61823	0.709287
7.13713	0.861944	18.074551	0.698836
7.14426	0.861869	18.30271	0.693337
7.15139	0.861794	18.53087	0.68763
7.16565	0.861644	18.759031	0.681694
7.17991	0.861494	18.987191	0.6755
7.20843	0.861193	19.21535	0.669017
7.23695	0.860892	19.44351	0.662203
7.29399	0.860289	19.671671	0.65496
7.35103	0.859684	19.89983	0.647297
7.46511	0.858469	20.12799	0.639089
7.57919	0.857249	20.24207	0.634744
7.80735	0.854789	20.35615	0.630213
8.03551	0.852304	20.470231	0.62547
8.49183	0.847255	20.584311	0.620485
8.94815	0.842096	20.698391	0.61522
9.86079	0.831427	20.81247	0.609625
10.77343	0.820243	20.92655	0.603632
11.686071	0.808479	21.04063	0.597148
12.59871	0.796055	21.097671	0.593681
13.51135	0.782868	21.15471	0.590037
13.96767	0.77595	21.21175	0.586187
14.42399	0.76879	21.268791	0.582092
14.880309	0.761364	21.32583	0.57764
15.33663	0.753646	21.382871	0.572848
15.79295	0.745604	21.43991	0.567562
16.249271	0.737199		
16.70559	0.728386		
17.161911	0.719105		

Table C 1.3: Bus 27 (EPZ)

Active power MW	voltage p.u	Active power MW	voltage p.u	Active power MW	voltage p.u
32.58	0.904982	88.84567	0.761358	113.4761	0.593547
32.61258	0.904922	90.93078	0.753267	113.6065	0.590275
32.64516	0.904861	93.01591	0.744753	113.7368	0.586657
32.67774	0.904801	95.10102	0.735755	113.8671	0.582511
32.7429	0.904679	97.18615	0.726192		
32.80806	0.904558	99.27126	0.715946		
32.93838	0.904316	100.3138	0.710529		
33.0687	0.904073	101.3564	0.704886		
33.32934	0.903587	102.3989	0.698987		
33.58998	0.903099	103.4415	0.692798		
34.11126	0.902121	104.4841	0.686276		
34.63254	0.901139	105.5266	0.679366		
35.6751	0.899162	106.5692	0.671996		
36.71766	0.897167	107.6117	0.66407		
38.80278	0.893124	108.133	0.659858		
40.8879	0.889006	108.6543	0.65545		
45.05814	0.880534	109.1756	0.65082		
49.22838	0.871725	109.6969	0.645932		
53.39863	0.862547	110.2181	0.64074		
57.56886	0.852962	110.7394	0.635185		
61.7391	0.842925	111.2607	0.629183		
65.90934	0.832383	111.782	0.622592		
70.07959	0.82127	112.0426	0.61903		
74.24983	0.809503	112.3033	0.615244		
78.42007	0.79698	112.5639	0.611187		
80.50518	0.790395	112.8245	0.606793		
82.59031	0.783566	113.0852	0.601966		
84.67542	0.77647	113.2155	0.599346		
86.76055	0.769079	113.3458	0.596552		

Table C 1.4:

Bus 51 (Kileleshwa)

ACTIVE POWER MW	VOLTAGE P.U
17.2500	0.9019
17.2673	0.9018
17.2845	0.9018
17.3018	0.9018
17.3363	0.9017
17.3707	0.9016
17.4398	0.9015
17.5088	0.9014
17.6468	0.9011
17.7848	0.9008
18.0608	0.9003
18.3367	0.8998
18.8888	0.8987
19.4408	0.8977
20.5448	0.8955
21.6488	0.8934
23.8568	0.8890
26.0648	0.8846
30.4807	0.8755
34.8968	0.8661
39.3128	0.8563
43.7288	0.8461
48.1447	0.8355
52.5607	0.8245
56.9768	0.8129
61.3928	0.8007
65.8088	0.7878
68.0168	0.7810
70.2248	0.7741
74.6408	0.7594

76.8487	0.7516
79.0568	0.7435
81.2647	0.7350

C 2. THE INCREMENTAL REACTIVE LOAD VARIATIONS GENERATED IN POWERFACTORY DiGSILENT

Table C 2.1: Bus 55 (Karen)

voltage p.u	Reactive Power MVAr	voltage p.u	Reactive Power MVAr
0.919	0.000	0.649	-41.285
0.909	-2.222	0.639	-42.087
0.899	-4.389	0.629	-42.839
0.889	-6.502	0.619	-43.541
0.879	-8.560	0.609	-44.193
0.869	-10.565	0.599	-44.795
0.859	-12.515	0.589	-45.346
0.849	-14.411	0.579	-45.848
0.839	-16.254	0.569	-46.301
0.829	-18.043	0.559	-46.704
0.819	-19.779	0.549	-47.057
0.809	-21.462	0.539	-47.361
0.799	-23.092	0.529	-47.616
0.789	-24.669	0.519	-47.822
0.779	-26.193	0.509	-47.980
0.769	-27.665		
0.759	-29.084		
0.749	-30.451		
0.739	-31.766		
0.729	-33.030		
0.719	-34.241		
0.709	-35.401		
0.699	-36.509		
0.689	-37.566		
0.679	-38.572		
0.669	-39.527		
0.659	-40.431		

Table C 2.2: Bus 42 (Magadi)

voltage p.u	Reactive Power MVAr	voltage p.u	Reactive Power MVAr
0.862	0.000	0.542	-14.683
0.852	-0.777	0.532	-14.816
0.842	-1.533	0.522	-14.929
0.832	-2.267	0.512	-15.024
0.822	-2.981	0.502	-15.100
0.812	-3.673		
0.802	-4.344		
0.792	-4.994		
0.782	-5.624		
0.772	-6.233		
0.762	-6.821		
0.752	-7.388		
0.742	-7.935		
0.732	-8.462		
0.722	-8.968		
0.712	-9.454		
0.702	-9.920		
0.692	-10.366		
0.682	-10.791		
0.672	-11.197		
0.662	-11.583		
0.652	-11.949		
0.642	-12.295		
0.632	-12.621		
0.622	-12.928		
0.612	-13.215		
0.602	-13.483		
0.592	-13.731		
0.582	-13.960		
0.572	-14.170		
0.562	-14.360		
0.552	-14.531		

Table C 2.3: Bus 27 (EPZ)

voltage p.u	Reactive Power MVAr	voltage p.u	Reactive Power MVAr
0.905	0.000	0.575	-75.700
0.895	-3.811	0.565	-76.416
0.885	-7.524	0.555	-77.042
0.875	-11.141	0.545	-77.576
0.865	-14.661	0.535	-78.019
0.855	-18.085	0.525	-78.371
0.845	-21.413		
0.835	-24.645		
0.825	-27.781		
0.815	-30.822		
0.805	-33.768		
0.795	-36.619		
0.785	-39.375		
0.775	-42.036		
0.765	-44.603		
0.755	-47.076		
0.745	-49.455		
0.735	-51.741		
0.725	-53.932		
0.715	-56.031		
0.705	-58.036		
0.695	-59.948		
0.685	-61.768		
0.675	-63.495		
0.665	-65.129		
0.655	-66.671		
0.645	-68.121		
0.635	-69.479		
0.625	-70.745		
0.615	-71.919		
0.605	-73.001		
0.595	-73.992		
0.585	-74.892		

Table C 2.4: Bus 51 (Kileleshwa)

Voltage (p.u)	Reactive Power (MVAr)	Voltage (p.u)	Reactive Power (MVAr)
0.910	0.000	0.590	-97.045
0.900	-4.914	0.580	-98.128
0.890	-9.704	0.570	-99.096
0.880	-14.369	0.560	-99.949
0.870	-18.911	0.550	-100.69
0.860	-23.329	0.540	-101.31
0.850	-27.624	0.530	-101.83
0.840	-31.796	0.520	-102.22
0.830	-35.846	0.510	-102.51
0.820	-39.773		
0.810	-43.578		
0.800	-47.262		
0.790	-50.825		
0.780	-54.266		
0.770	-57.586		
0.760	-60.787		
0.750	-63.866		
0.740	-66.826		
0.730	-69.667		
0.720	-72.388		
0.710	-74.990		
0.700	-77.474		
0.690	-79.839		
0.680	-82.086		
0.670	-84.216		
0.660	-86.227		
0.650	-88.122		
0.640	-89.900		
0.630	-91.561		
0.620	-93.106		
0.610	-94.535		
0.600	-95.848		

APPENDIX D

LOAD BUS BASE OPERATING VOLTAGES

Table D: The load bus operating voltages

BUS NO	10	19	22	24	26	27	29
BUS NAME	Juja Rd	Naivasha	Baba Dogo	Steel Billets	Parklands	EPZ	Thika
VOLTAGE (P.U)	0.995	1.017	1.002	1.008	0.967	0.905	0.932
BUS NO	31	32	33	34	35	36	37
BUS NAME	Nbi west	Matasia	Athi River	Airport	NSSF	Msa Rd	Limuru
VOLTAGE (P.U)	0.965	0.962	0.977	0.997	0.983	1	0.959
BUS NO	38	39	40	41	42	43	44
BUS NAME	Ruaraka	Ruiru	Cianda	Kitsuru	Magadi	Jeevanjee	Westlands
VOLTAGE (P.U)	0.95	0.996	0.999	0.985	0.862	1	0.993
BUS NO	45	46	48	49	50	51	53
BUS NAME	KPC, Nbi	Cathedral	Kikuyu	Ngong Rd	Kimathi	Kileleshwa	New Ind
VOLTAGE (P.U)	1.01	0.964	0.934	0.908	1	0.901	0.981
BUS NO	54	55	56	57	58		
BUS NAME	Firestone	Karen	KPC Ngema	Gigiri Water	Morris & Co.		
VOLTAGE (P.U)	0.992	0.919	0.955	0.983	1.01		

APPENDIX E

NETWORK LOAD BUS SENSITIVITY FACTORS

Table E: Load bus sensitivity Factors

Bus No	42	55	27	48	32	57	29
Bus Name	Magadi	Karen	KPZ	Kikuyu	Matasia	Gigiri W/W	Thika
Sensitivity	0.7696	0.4925	0.354	0.3301	0.2832	0.2755	0.2672
Bus No	41	56	49	51	44	38	26
Bus Name	Kitsuru	KPC Ngema	Ngong Road	Kileleshwa	Westland	Ruiiru Steel	Parkland
Sensitivity	0.2238	0.2224	0.189	0.1889	0.1857	0.1844	0.1814
Bus No	37	40	47	20	39	28	15
Bus Name	Limuru	Cianda	Ngong Rd Junction	Nairobi North 66KV	Ruaraka	Thika/ Tana Junction	Ruaraka 66kV
Sensitivity	0.171	0.1569	0.1193	0.1059	0.0887	0.087	0.0866
Bus No	33	53	50	35	43	46	22
Bus Name	Athi River	New Industrial	Kimathi	NSSF	Jeevanjee	Cathedral	Baba Dogo
Sensitivity	0.0794	0.0789	0.0757	0.0637	0.0624	0.0605	0.0561
Bus No	31	54	19	25	52	58	11
Bus Name	Nairobi West	Fire Stone	Naivasha 132kV	Kimathi Junction	Firestone Juntion	Morris & Co.	Ruaraka 132kV
Sensitivity	0.0506	0.0421	0.0377	0.0373	0.0312	0.0308	0.0241
Bus No	24	21	34	9	10	45	5
Bus Name	EMCO	Ruaraka Junction	New Airport	Dandora 132kV	Juja Rd 132kV	KPC Nairobi	Nairobi North 220kV
Sensitivity	0.0234	0.0223	0.022	0.0189	0.0179	0.0151	0.0147
Bus No	3	4	14	17	2	36	
Bus Name	Embakasi 220kV	Dandora 220kV	Juja Rd 66kV	Olkaria II 132kV	Kamburu 220kV	Mombasa Rd	
Sensitivity	0.0146	0.0128	0.0124	0.0069	0.0054	0.002	

APPENDIX F

NETWORK MODAL EIGENVALUES

Table F: Modal Eigenvalues

Mode	30	39	40	32	33	38	31
Eigenvalue	0.7	1.1	2.2	2.6	2.9	2.9	3.4
Mode	34	35	44	37	45	36	43
Eigenvalue	5.2	5.8	6.9	7.5	8.4	10	12.6
Mode	42	48	46	47	41	29	28
Eigenvalue	14.6	14.9	15.7	16	16.2	18.5	19.2
Mode	26	25	27	23	22	24	21
Eigenvalue	21.5	23.3	25	30.6	31.9	34.3	37
Mode	19	20	17	18	16	15	13
Eigenvalue	43.2	45.5	51.3	57.5	58.7	89	128.8
Mode	12	9	14	7	11	8	10
Eigenvalue	144.6	161.5	168.4	191.4	215.2	215.3	227.4
Mode	6	5	4	2	3	1	
Eigenvalue	336.7	499.7	586.5	945.8	1012.3	1252.1	

APPENDIX G

BUS PARTICIPATION FACTORS

Table G 1.1: Bus Participation Factorsin Mode 30

BUS NO	55	48	56	37	57	41	44
PART, FACTOR	0.2426	0.184	0.1078	0.0995	0.0931	0.0859	0.065
BUS NO	40	20	5	4	3	15	38
PART, FACTOR	0.0615	0.0565	0.0014	0.0008	0.0006	0.0002	0.0002
BUS NO	39	9	10	11	21	27	2
PART, FACTOR	0.0002	0.0001	0.0001	0.0001	0.0001	0.0001	0
BUS NO	14	17	19	22	24	25	26
PART, FACTOR	0	0	0	0	0	0	0
BUS NO	28	29	31	32	33	34	35
PART, FACTOR	0	0	0	0	0	0	0
BUS NO	36	42	43	45	46	47	49
PART, FACTOR	0	0	0	0	0	0	0
BUS NO	50	51	52	53	54	58	
PART, FACTOR	0	0	0	0	0	0	

Table G 1.2: Bus Participation Factors in Mode 39

BUS NO.	42	32	2	3	4	5	9
PART.FACTOR	0.8195	0.1805	0	0	0	0	0
BUS NO.	10	11	14	15	17	19	20
PART.FACTOR	0	0	0	0	0	0	0
BUS NO.	21	22	24	25	26	27	28
PART.FACTOR	0	0	0	0	0	0	0
BUS NO.	29	31	33	34	35	36	37
PART.FACTOR	0	0	0	0	0	0	0
BUS NO.	38	39	40	41	43	44	45
PART.FACTOR	0	0	0	0	0	0	0
BUS NO.	46	47	48	49	50	51	52
PART.FACTOR	0	0	0	0	0	0	0
BUS NO.	53	54	55	56	57	58	
PART.FACTOR	0	0	0	0	0	0	

Table G 1.3: Bus Participation Factors in Mode 40

BUS NO.	51	49	47	46	31	2	3	4	5	9
PART, FACTOR	0.3258	0.3252	0.2322	0.0598	0.057	0	0	0	0	0
BUS NO.	10	11	14	15	17	19	20	21	22	24
PART, FACTOR	0	0	0	0	0	0	0	0	0	0
BUS NO.	25	26	27	28	29	32	33	34	35	36
PART, FACTOR	0	0	0	0	0	0	0	0	0	0
BUS NO.	37	38	39	40	41	42	43	44	45	48
PART, FACTOR	0	0	0	0	0	0	0	0	0	0
BUS NO.	50	52	53	54	55	56	57	58		
PART, FACTOR	0	0	0	0	0	0	0	0		

Table G 1.4: Bus Participation Factors in Mode 32

BUS NO	27	38	29	39	15	28	11
PART. FACTORS	0.4229	0.1935	0.1218	0.0942	0.0929	0.0241	0.01
BUS NO	21	10	26	50	43	25	19
PART. FACTORS	0.0087	0.0053	0.0053	0.0025	0.0023	0.002	0.0017
BUS NO	57	22	24	14	41	55	4
PART. FACTORS	0.0016	0.0015	0.0012	0.0011	0.0011	0.0004	0.0003
BUS NO	3	5	20	40	44	48	2
PART. FACTORS	0.0002	0.0002	0.0001	0.0001	0.0001	0.0001	0
BUS NO	17	31	32	33	34	35	36
PART. FACTORS	0	0	0	0	0	0	0
BUS NO	37	42	45	46	47	49	51
PART. FACTORS	0	0	0	0	0	0	0
BUS NO	52	53	54	56	58		
PART. FACTORS	0	0	0	0	0		

Table G 1.5: Bus Participation Factors in Mode 33

BUS NO	27	38	55	39	15	29	57
PART. FACTOR	0.4405	0.098	0.062	0.0554	0.0548	0.0503	0.037
BUS NO	41	48	26	28	50	11	43
PART. FACTOR	0.0279	0.0232	0.0218	0.0144	0.0127	0.0118	0.0118
BUS NO	21	25	10	22	9	24	14
PART. FACTOR	0.0109	0.0102	0.0086	0.0083	0.0082	0.0069	0.0064
BUS NO	44	40	20	19	4	5	3
PART. FACTOR	0.006	0.005	0.0038	0.002	0.0008	0.0007	0.0006
BUS NO	2	17	31	32	33	34	35
PART. FACTOR	0	0	0	0	0	0	0
BUS NO	36	37	42	45	46	47	49
PART. FACTOR	0	0	0	0	0	0	0
BUS NO	51	52	53	54	56	58	
PART. FACTOR	0	0	0	0	0	0	

Table G 1.6: Bus Participation Factors in Mode 38

Bus	27	38	29	15	39	11	21
Participation Factor	0.9973	0.0008	0.0006	0.0004	0.0004	0.0001	0.0001
Bus	26	28	2	3	4	5	9
Participation Factor	0.0001	0.0001	0	0	0	0	0
Bus	10	14	17	19	20	22	24
Participation Factor	0	0	0	0	0	0	0
Bus	25	31	32	33	34	35	36
Participation Factor	0	0	0	0	0	0	0
Bus	37	40	41	42	43	44	45
Participation Factor	0	0	0	0	0	0	0
Bus	46	47	48	49	50	51	52
Participation Factor	0	0	0	0	0	0	0
Bus	53	54	55	56	57	58	
Participation Factor	0	0	0	0	0	0	

APPENDIX H

LINEAR BUS REACTIVE POWERS

Table H 1: Linear bus reactive powers for buses in mode 30

BUS NO.	3.000	4.000	5.000	9.000	10.000	11.000	15.000	20.000
LINEAR REACTIVE POWERS	-0.025	-0.025	-0.037	-0.012	-0.011	-0.011	-0.013	-0.238
BUS NO	21.000	37.000	38.000	39.000	40.000	41.000	44.000	48.000
LINEAR REACTIVE POWERS	-0.011	-0.316	-0.014	-0.013	-0.248	-0.293	-0.255	-0.429
BUS NO	55.000	56.000	57.000					
LINEAR REACTIVE POWERS	-0.493	-0.328	0.305					

Table H 2: Linear bus reactive powers for

buses in mode 39

BUS NO	32	42
LINEAR REACTIVE POWERS	1.0708	1.3895

Table H 3: Linear bus reactive powers for buses in mode 40

BUS NO	31	46	47	49	51
LIEAR REACTIVE POWERS	-3.11E-14	-1.92E-13	-8.39E-16	1.01E-14	1.17E-14

Table H 4:Linear bus reactive powers for buses in mode 32

BUS	15	38
LINEAR REACTIVE POWERS	1.5843	1.4546

APPENDIX J

LINEAR BRANCH REACTIVE POWER LOSSES

Table J 1: The linear branch reactive power losses for branches in mode 30

BRANCH	3-4	4-5	9-10	10-21	11-21	15 - 38	15 - 39	20 - 40
LINEAR REACTIVE POWER LOSSES	-0.0002	-0.012	-0.0009	-0.0002	-1.00E-04	-0.0011	0	-0.0103
BRANCH	20 - 37	20 - 44	20 - 41	37- 56	37 - 48	48 - 55	41 - 57	
LINEAR REACTIVE POWER LOSSES	-0.0778	-0.0172	-0.0554	-0.0128	-0.1134	-0.0637	-0.012	

Table J 2: The linear branch reactivePower losses in mode 39

BRANCH	32-42
LINEAR REACTIVE POWER LOSS	0.3187

Table J 3: The linear bus reactive power losses in mode 40

BRANCH	31-46	31-47	47-49	47-51
LINEAR REACTIVE POWER LOSSES	-1.61E-13	3.03E-14	1.09E-14	1.26E-14

Table J 4: The linear branch reactive Power losses in mode 32

BRANCH	15-38
LINEAR REACTIVE POWER LOSS	-0.1297